AD-A104 248   DEFENCE RESEARCH ESTABLISHMENT OTTAWA (ONTARIO)   F/G 18/8
              A COMPARISON OF MEASURED AND CALCULATED AIR-TRANSPORTED RADIATI--ETC(U)
              DEC 80   H A ROBITAILLE, B E HOFFARTH
UNCLASSIFIED DREO-R-835   NL
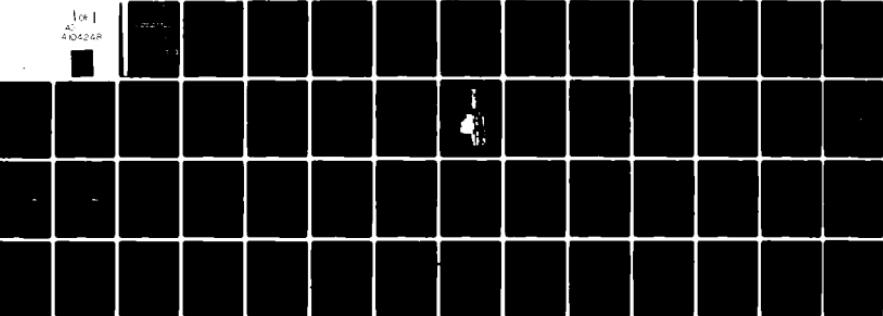
1 of 1
AD
A104248

END
DATE
FILMED
10-81
DTIC

③ LEVEL II

AD A104248

RESEARCH AND DEVELOPMENT BRANCH
DEPARTMENT OF NATIONAL DEFENCE
CANADA

DEFENCE RESEARCH ESTABLISHMENT OTTAWA

DREO REPORT NO. 835
DREO R 835

A COMPARISON OF MEASURED AND CALCULATED AIR-TRANSPORTED RADIATION FROM A FAST, UNSHIELDED NUCLEAR REACTOR

by

H. A. Robitaille and B. E. Hoffarth

DTIC
ELECTE
SEP 1 5 1981
B

PROJECT NO.
SPN 11A10-1

DECEMBER 1980
OTTAWA

DTIC FILE COPY

RESEARCH AND DEVELOPMENT BRANCH

DEPARTMENT OF NATIONAL DEFENCE
CANADA

DEFENCE RESEARCH ESTABLISHMENT OTTAWA

REPORT NO. 835

A COMPARISON OF MEASURED AND CALCULATED AIR-TRANSPORTED RADIATION FROM A FAST, UNSHIELDED NUCLEAR REACTOR,

by

H. A. Robitaille and B. E. Hoffarth

Nuclear Effects Section
Protective Sciences Division

PROJECT NO.
SPN 11A10-1

DECEMBER 1980
OTTAWA

ABSTRACT

Neutron and gamma-ray spectra have been measured at various distances up to 1100 metres from the fast-neutron reactor of the U.S. Army Pulse Radiation Division (Materiel Testing Directorate, Aberdeen Proving Ground, Md.) The spectra were obtained at a height of two metres above the air-ground interface and are compared to previous measurements performed by two other research laboratories, and also to the results of theoretical predictions based on two-dimensional discrete-ordinates transport theory.

Integral quantities such as partial and total radiation kermas are generally in good agreement, however the theoretical calculations tend to predict somewhat softer neutron spectra than are observed experimentally.

RÉSUMÉ

On a measuré des spectres de rayons gamma et de neutrons à différentes distances jusqu'à 1100 mètres du réacteur nùcléaire à neutrons rapides de la Pulse Radiation Division de la U.S. Army (Materiel Testing Directorate, Aberdeen Proving Ground, Md.). Ils ont été obtenus à une hauteur de deux mètres au-dessus de l'interface air-sol; on a comparé ces spectres à des mesures antérieures effectuées par deux autres laboratoires de recherche, de même qu'à des résultats de prévisions théoriques découlant d'une théorie du transport bidimensionnelle à ordonnées discrètes.

Des quantités intégrales comme les kermas de rayonnement partiels et totaux concordent de façon générale avec les observations expérimentales, cependant les calculs théoriques ont tendance à prédire des spectres de neutrons moins énergétiques.

CONTENTS

v/vi

ILLUSTRATIONS

TABLES

INTRODUCTION

This report describes the results of experiments performed by DREO personnel at the U.S. Army Pulse Radiation Division (Aberdeen Proving Ground, Aberdeen, Maryland) during the period 6 Oct to 17 Oct 1980. The object of the experiments was to provide sufficient information for the critical evaluation of the accuracy of theoretical predictions of the transport of neutron and gamma-ray radiation through the atmosphere.

The source of radiation was a fast-neutron, unmoderated and unshielded, GODIVA-type nuclear reactor positioned at a height of 14 metres above ground level, and relatively unperturbed by surrounding structures. Neutrons and gamma-rays were measured at a height of 2 metres above ground using an NE-213 spectrometer and Boron-trifluoride counters. Spectra were obtained at ground ranges of 15, 100, 170, 300, 400, and 1100 metres from the reactor.

In addition, a corresponding theoretical calculation was made using a two-dimensional, discrete-ordinates transport model, identical to that used for previous calculations of the free-field radiation environments surrounding tactical nuclear weapons detonated in air-over-ground and air-over-seawater geometries (1). The measured spectra were compared to these predictions to determine the applicability of the transport model to the nuclear weapons problem.

THE APRD REACTOR

The US APRD reactor is a fast-burst bare assembly of 106 kg uranium-molybdenum (90:10) alloy fuel, enriched to 92 % in uranium-235, in the form of a right circular cylinder (2). The reactor is of the GODIVA-type design, based on the Health Physics Research Reactor at the Oak Ridge National Laboratory. At the maximum steady-state continuous power level of four kilowatts, the reactor releases neutrons at the rate of 1.4×10^{14} per second and gamma-rays at 9.2×10^{13} per second (3). Due to the high enrichment and small physical size of the core (226 mm diameter x 198 mm height), the spectrum of leakage neutrons is perturbed minimally from that due to the fission process, and thus serves as an excellent simulator of nuclear weapon radiation. The core may be positioned both within and outside a low-scattering aluminum weather-protecting silo by means of a remotely-controlled transporter. During these experiments the reactor was located as far from the silo as possible and at a height of 14 metres above ground level.

Normalization of measured data to the neutron production rate was made on the basis of time and power level, employing a calibration factor of 1.28×10^{17} neutrons per kilowatt-hour (3). Details of the neutron and gamma-ray leakage spectra are taken directly from reference 3, and listed in Appendix I.

RADIATION DETECTORS

NE-213

Neutrons above 600 keV and gamma-rays above 300 keV in energy were detected using an NE-213 spectrometer system (4) using constant-fraction-timing pulse-shape discrimination. Pulse-height data were recorded for both neutrons and gamma-rays simultaneously at two amplification levels by a PDP-11/34 computer employing four separate analogue input channels with direct-memory-access interfacing. Data analysis was performed by an unfolding technique described elsewhere (5) using DREO calculated neutron response data (4) and gamma-ray response data due to Lurie, et al (6).

Neutron and gamma-ray kermas were determined by folding the measured spectra against the appropriate conversion factors (7) listed also in Appendix I.

Boron-trifluoride counters

At the ranges of interest in the air-over-ground problem, NE-213 spectrometers account for approximately 90 % of the kerma due to gamma rays and 65 % of that due to neutrons, due to the loss of information below the previously mentioned lower-energy thresholds. In order to determine the neutron kerma below 600 keV, a pair of matched boron-trifluoride neutron detectors (8) were incorporated into the detection system. One was operated "bare", the other encased in cadmium sheet of 0.102 cm thickness. As the alpha-producing absorption cross-section of boron-10 decreases rapidly with increasing neutron energy, both detectors are sensitive primarily to low-energy neutrons. The cadmium covering acts as a filter, allowing neutrons only above 0.5 eV (50 % transmission) to be detected by the lined counter. The difference in total counts registered in the two counters is thus in proportion to the thermal-neutron fluence (i.e. below 0.5 eV), which may be readily determined by dividing by the detector efficiency.

The distribution of neutrons above 0.5 eV is inferred from the cadmium-covered detector by assuming that the energy spectrum is reasonably well represented by a power curve of the form :

$$\emptyset \, (E) \; = \; A \, E^{p}$$

The parameters A and p are uniquely determined by requiring that the neutron spectrum at 800 keV is continuous in energy compared to the NE-213 determination, and that the total counts recorded are reproduced when the parametric spectrum is integrated against the energy-dependant detection efficiency. Although this is not strictly a spectroscopic measurement, derived integral quantities such as total fluence and/or various doses will be accurate provided the neutron spectrum into which the detectors are placed is free of significant structure below 600 keV.

Prior to use, the detectors were calibrated against the Canadian thermal-neutron standard (9,10), and a total boron-10 content of 9.11×10^{20} sensitive nuclei was determined for each detector.

EXPERIMENTAL MEASUREMENTS

Spectral data were obtained at the six ground ranges listed below, under weather conditions that were generally favourable and consistent over the two-week period of measurement.

Range (m)	Heights		Reactor Power (W)	Measurement Times		Atmospheric	
	Core (m)	Detector (m)		Foregnd (h)	Backgnd (h)	Density (g/1)	Humidity (%)
15	5.34	5.34	0.3	0.5	0.5	1.23	43
100	14	2	10	0.5	0.25	1.24	78
170	14	2	40	0.5	0.25	1.24	78
300	14	2	200	0.5	0.25	1.24	78
400	14	2	1000	0.5	0.25	1.26	50
1100	14	2	4000	5.0	0.5	1.23	62

Table 1 : Important reactor, detector and weather parameters at each point of measurement.

The core height of fourteen metres corresponds to the maximum capability of the transporter. At the fifteen-metre range it was desired to measure the leakage spectrum from the side of the core, therefore a height of 5.34 metres was chosen, as this was the maximum to which the detectors could be raised. At longer ranges a detector height of two metres was used in order to be consistent with previous measurements (3) by the Army Pulse Radiation Division (APRD), and the Wehrwissenschaftliche Dienststelle (WWD) of the Federal Republic of Germany (11).

Surrounding the reactor at approximately 200 metres is a fairly dense forest cover. At closer distances the terrain is smooth and cleared of all trees. A line-of-sight path of twenty metres in width extends further to a distance of 450 metres total. The measurements at 300 and 400 metres were made at the centreline of this path. At 1100 metres the detectors were placed atop a small hill of about 25 metres in height in order to maintain line-of-sight to the core above the forest cover.

For each measurement the reactor power level was chosen such that the dead-time associated with the most active channel was approximately 2 %. At the closest distance of 15 metres, this was impossible due to the very high gamma background from the residual activity of the core. Gamma-ray measurements proved to be impractical at this range since a power level sufficient to overcome the gamma-ray background would result in prohibitive dead-times. The dead-times associated with the neutron channels were, however, within the 2 % criterion.

In the worst case (gamma-rays at 1100 metres), the ratio of foreground to background counting rates was 5.8 to 1. A total run time of 5 hours was therefore required to ensure an adequate statistical accuracy of 0.13 % in the expected error of the difference between total counts. A minimum of 500,000 counts was recorded at each position for each of the neutron and gamma-ray spectra. In most cases the actual net number of particles observed exceeded 2,000,000, as is shown in Table 2.

Range	Foreground Rate		Background Rate		Net Observed Particles	
(m)	Neutron	Gamma	Neutron	Gamma	Neutron	Gamma-ray
15	2906	–	61.9	–	5,119,000	–
100	1564	1644	0.21	216	2,815,000	2,570,000
170	1702	2043	0.11	116	3,063,000	3,469,000
300	1171	2040	0.05	72	2,108,000	3,542,000
400	1921	3660	0.04	96	3,458,000	6,415,000
1100	29.3	131	0.03	22.4	527,000	1,955,000

Table 2 : Foreground and background counting rates (per second), and net particles observed at each measurement position.

EXPERIMENTAL RESULTS

Neutron and Gamma-ray Spectra

Measured neutron and gamma-ray spectra, after unfolding, were integrated into the energy groups of the DLC-31 data-library structure (7), as listed in Appendix I. This format includes 37 groups for neutrons and 21 for gamma-rays, and is used primarily to facilitate the comparison of measured spectra with corresponding theoretical predictions. Figures 1 and 2 show the measured neutron and gamma-ray spectra in the multi-group format and normalized per source neutron. Note that the plotted variable in both cases is the fluence per unit lethargy, obtained by dividing the group-wise fluences by their respective lethargy-increments (natural logarithms of the ratios of group energy bounds). The portions of the neutron spectra above 600 keV were obtained from the NE-213 measurements, and as previously indicated below this energy from the parametric BF3 determinations. In Appendix II are listed the group fluences for both neutrons and gamma rays, in the DLC-31 format.

As the BF3 parameters are an indication of the approach of the neutron spectrum to a well-moderated asymptotic behaviour of $1/E$, it is interesting to examine their change with distance. Listed below are the parameters A and p inferred at the six measurement positions.

Range (m)	A	p
15	1.57 E- 8	-0.769
100	2.76 E-10	-0.886
170	7.58 E-11	-0.913
300	1.02 E-11	-0.942
400	3.37 E-12	-0.956
1100	1.24 E-14	-0.975

Table 3 : Epithermal neutron parameters inferred from BF3 data.

The magnitude A is scaled such that the parametric formula $\emptyset = AE^p$ reproduces the epithermal neutron spectrum in units of neutrons per $(cm^2 \cdot MeV \cdot source$ neutron$)$. As the ground range increases, it is apparent that the parameter p tends toward the value of -1, which would be characteristic of a fully moderated system (i.e. $1/E$ spectrum), as expected.

NEUTRON ENERGY, E_n (MeV)

NEUTRON FLUENCE, $E_n \phi_n(E_n)$ (cm^{-2})

15m

100m
170m
300m
400m

1100m

10^{-6}
10^{-8}
10^{-10}
10^{-12}
10^{-14}
10^{-16}

0   2   4   6   8   10   12
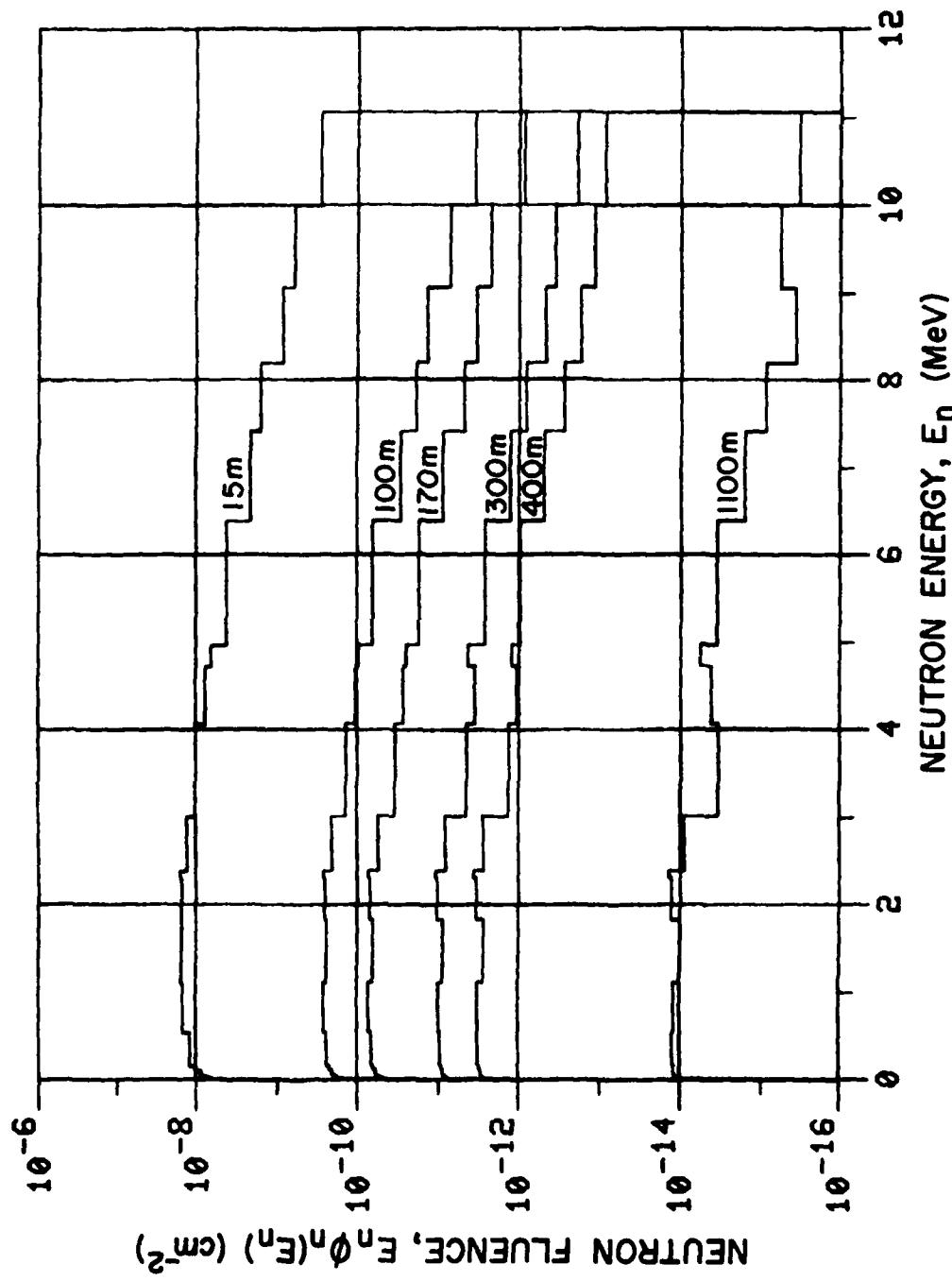
Figure 1 : DREO measured neutron spectra per source neutron regrouped in the DLC-31 data structure.

6
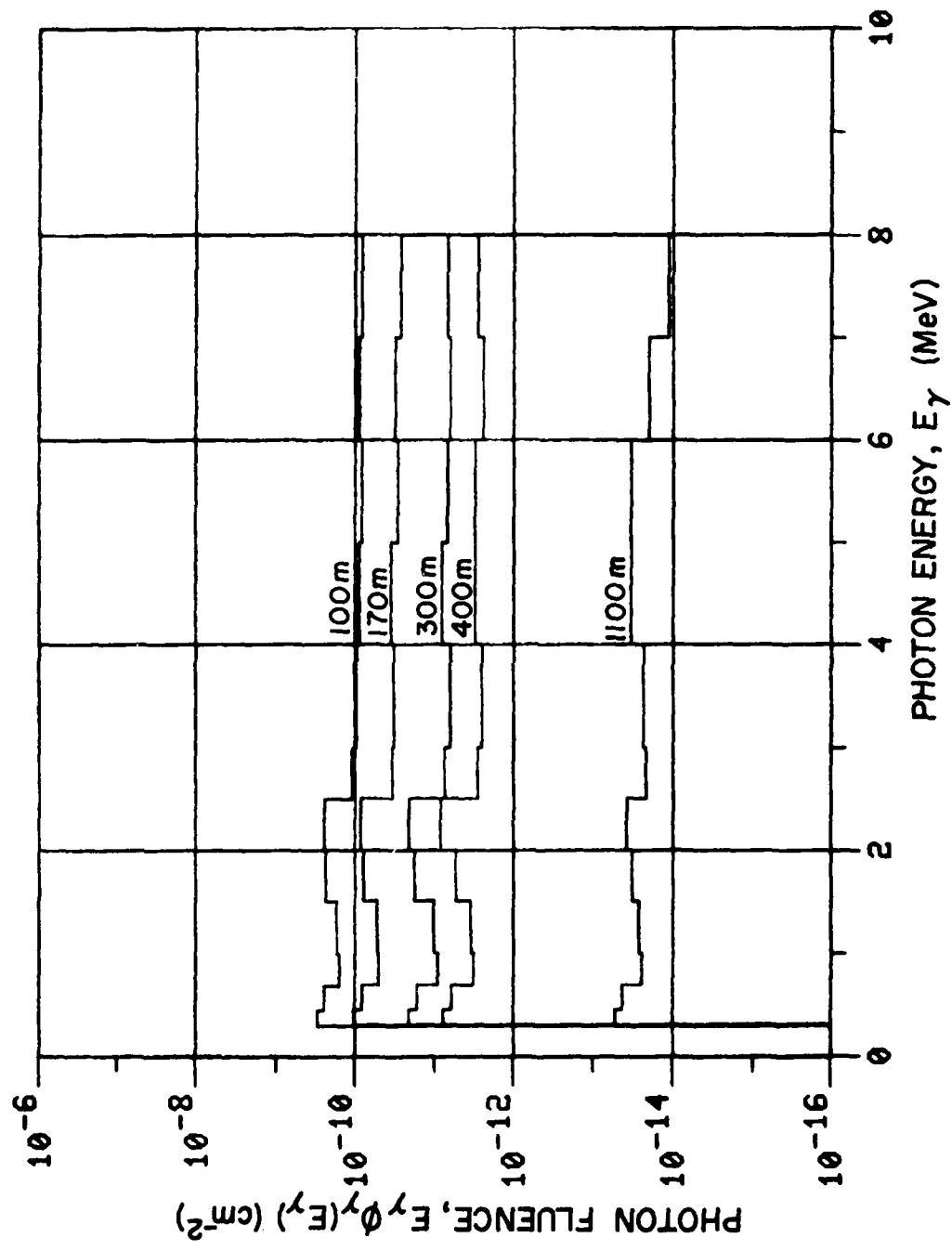
Figure 2 : DREO measured gamma-ray spectra per source neutron regrouped in the DLC-31 data structure.

Comparison to APRD and WWD Determinations

At ground ranges of 100, 170 and 300 metres previous measurements of neutron spectra had been made by APRD (3), and of both neutron and gamma-ray spectra by WWD (11). For each ground range and each particle type, comparisons of DREO measurements with these existing data are shown in Figures 3 through 8. Only DREO spectral data exist at ranges beyond 300 metres due to the uniqueness of the DREO mobile nuclear laboratory, based on a thirty-foot motorhome and self-contained with respect to power and environmental control (Plate 1).

Neutron spectra measured by the three groups agree reasonably well (Figures 3 to 5), within a typical scatter of about +/- 20 %. The APRD spectra tend to be consistently slightly greater than either the DREO or WWD data. The agreement above 2 MeV is generally better between DREO and WWD, with the DREO results most often between the data of the other two groups. Below a neutron energy of 2 MeV, the DREO data falls consistently below that of both APRD and WWD. The cause of this discrepancy is not entirely obvious, but one possibility is that it results from a difference in neutron response matrices used to unfold the measured spectra. Both APRD and WWD had previously found it necessary to modify their response matrices below 2 MeV in order to reproduce 252-californium fission-neutron spectra according to the accepted shape (12,13). The extent and direction of the re-normalization of response elements is consistent with the present difference of neutron spectra. Altough the DREO matrix shares a common ancestry, namely the OSS code (14), this re-normalization was never required, as is shown in Appendix IV. Another possibility is that due to differences in pulse-shape discrimination techniques, the three groups are not always consistent in their identification of particle type at low NE-213 light outputs. It is hoped that further inter-comparisons between APRD, WWD and DREO will eventually lead to a definitive explanation of the current discrepancy.

A comparison of DREO- and WWD-measured gamma-ray spectra (Figures 6 to 8) demonstrates fairly acceptable agreement, with some detail differences. Below 1 MeV, DREO data significantly exceeds that of WWD. Near 2.2 MeV (gamma-ray production following neutron capture by hydrogen) the WWD spectra show better resolution than those of DREO. Up to 6 MeV the agreement between the two groups is excellent. Between 6 and 8 MeV, DREO measured more photons than WWD but in excess of 8 MeV DREO measured fewer, although the total integral above 6 MeV is in close agreement. Many possible causes could be responsible for these differences, including unfolding procedures, post-unfolding smoothing, differences in lower detection thresholds, and/or gain calibrations. Another likely cause is differing soil water-content, since a significant fraction of gamma-rays detected at these ranges originate following neutron capture in the ground.
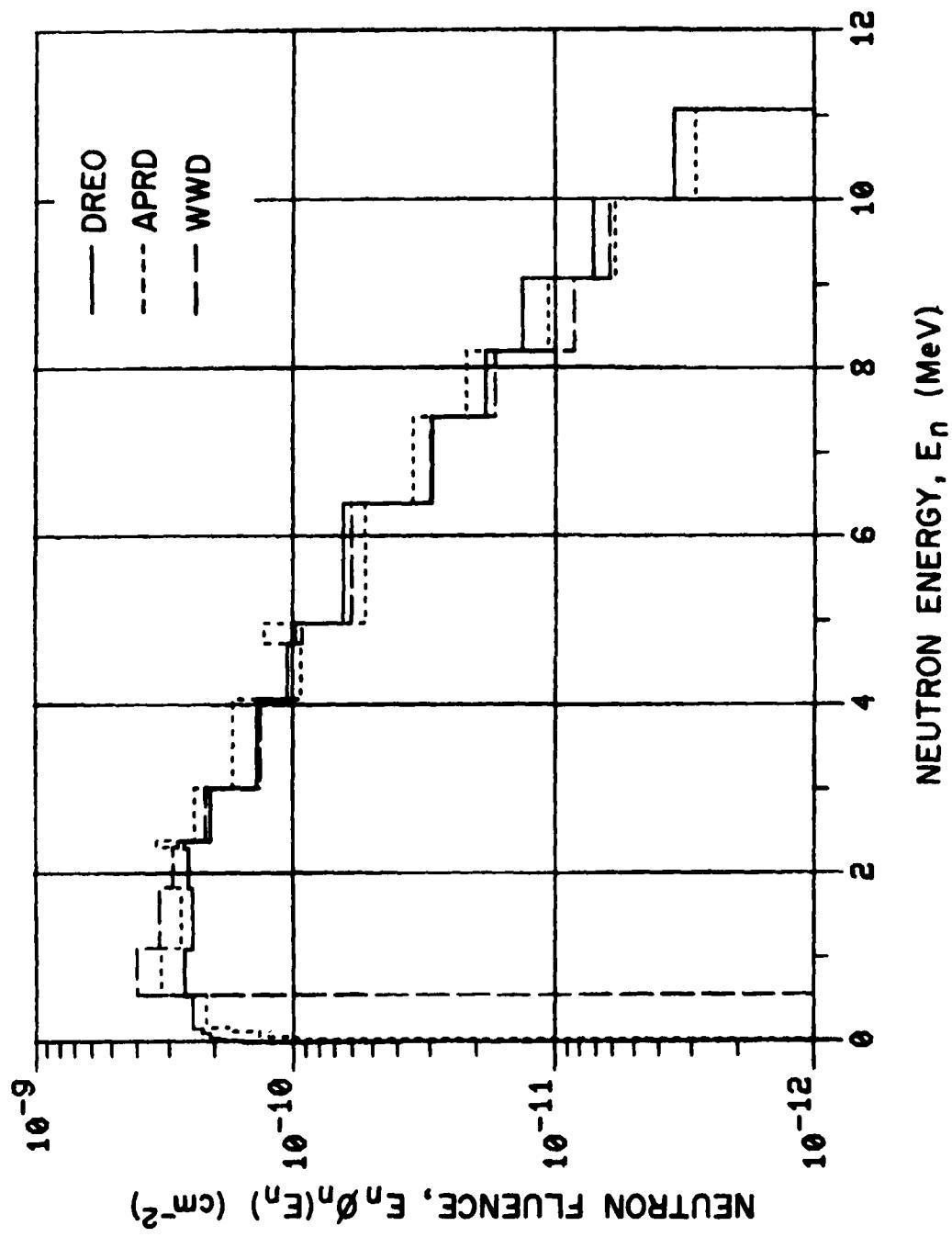
Figure 3 : Measured neutron spectra at a ground range of 100 metres.
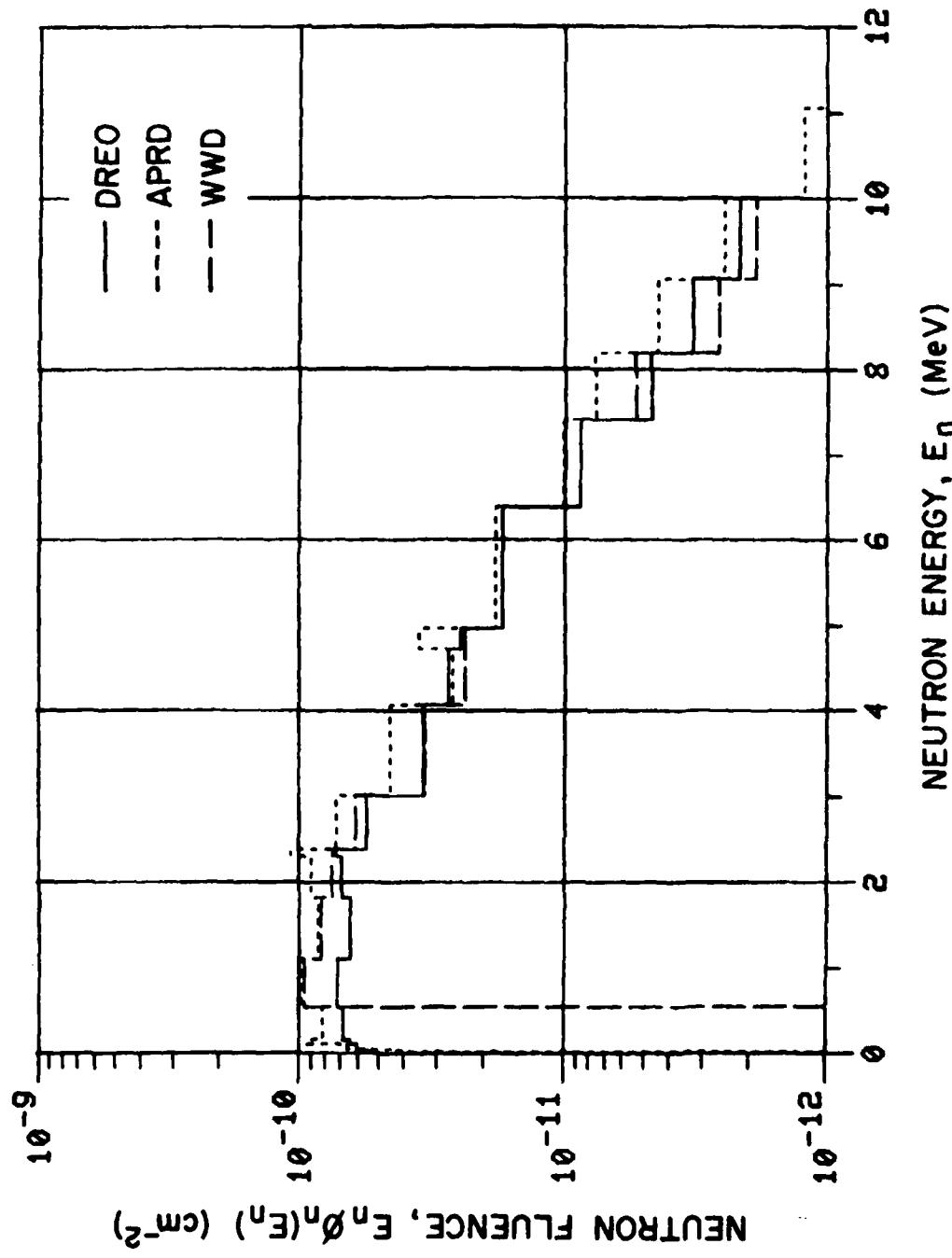
Figure 4 : Measured neutron spectra at a ground range of 170 metres.
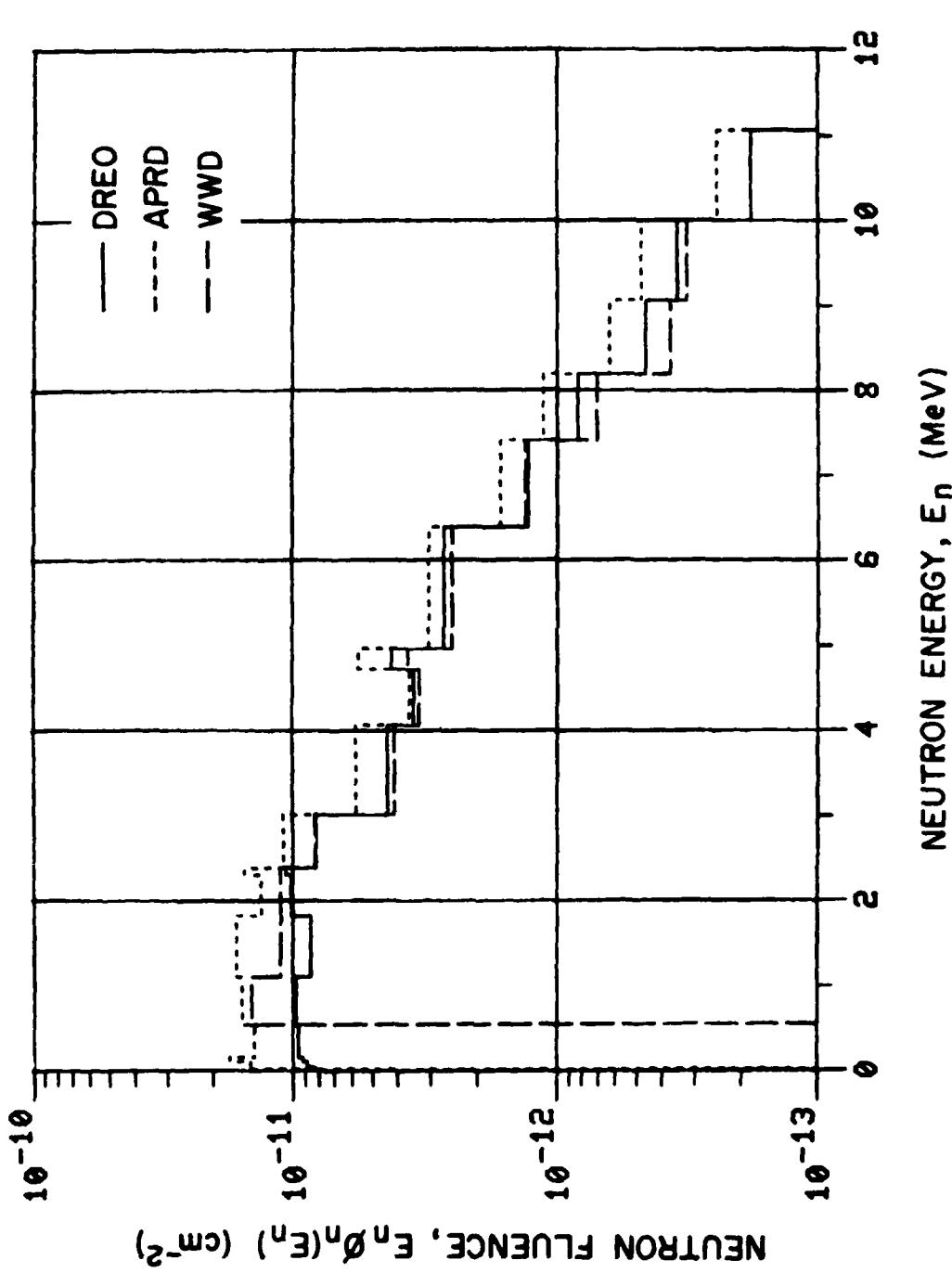
Figure 5 : Measured neutron spectra at a ground range of 300 metres.

11

PHOTON ENERGY, E_γ (MeV)

PHOTON FLUENCE, $E_\gamma \phi_\gamma(E_\gamma)$ (cm^{-2})
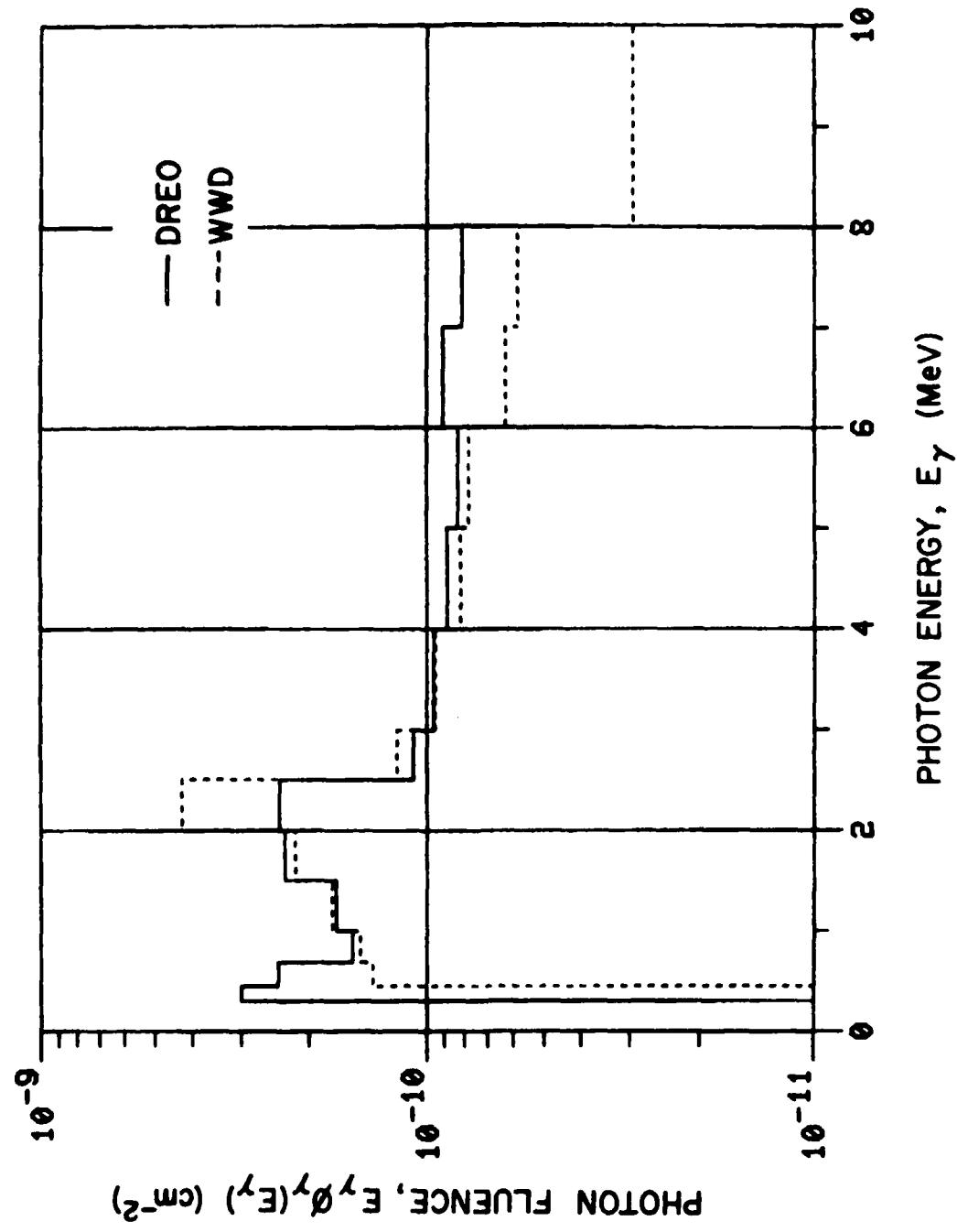
Figure 6 : Measured gamma-ray spectra at a ground range of 100 metres.
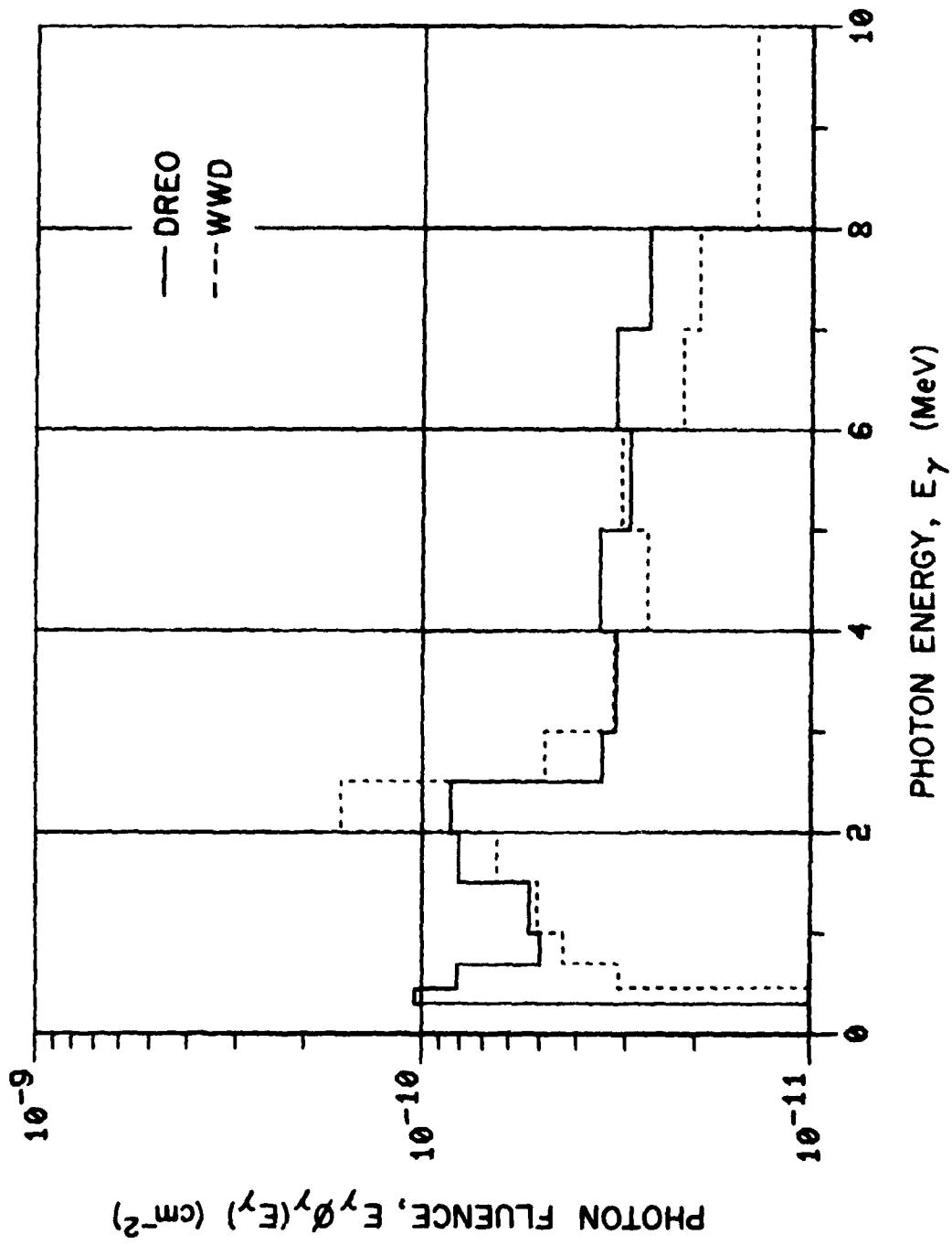
Figure 7 : Measured gamma-ray spectra at a ground range of 170 metres.
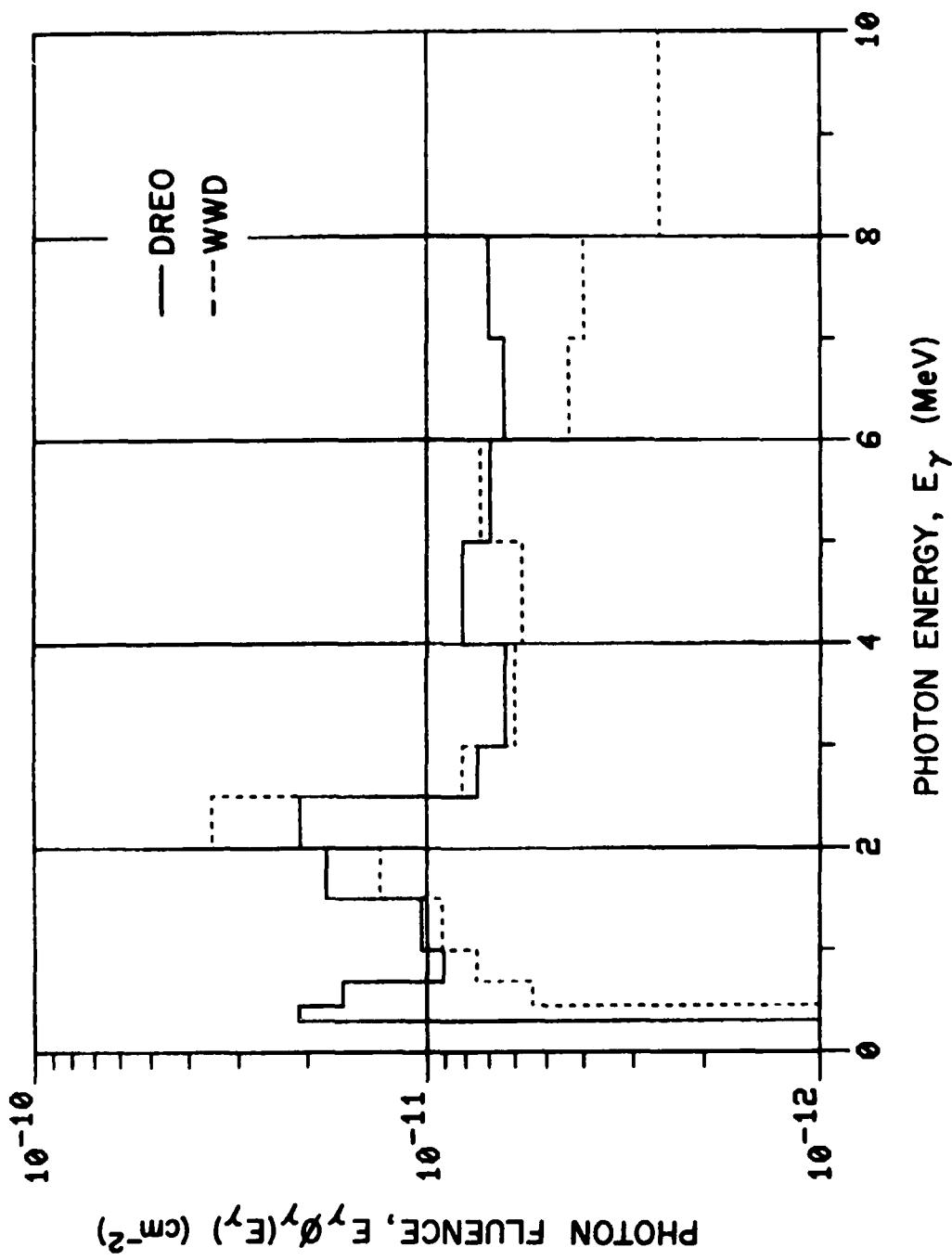
Figure 8 : Measured gamma-ray spectra at a ground range of 300 metres.

14
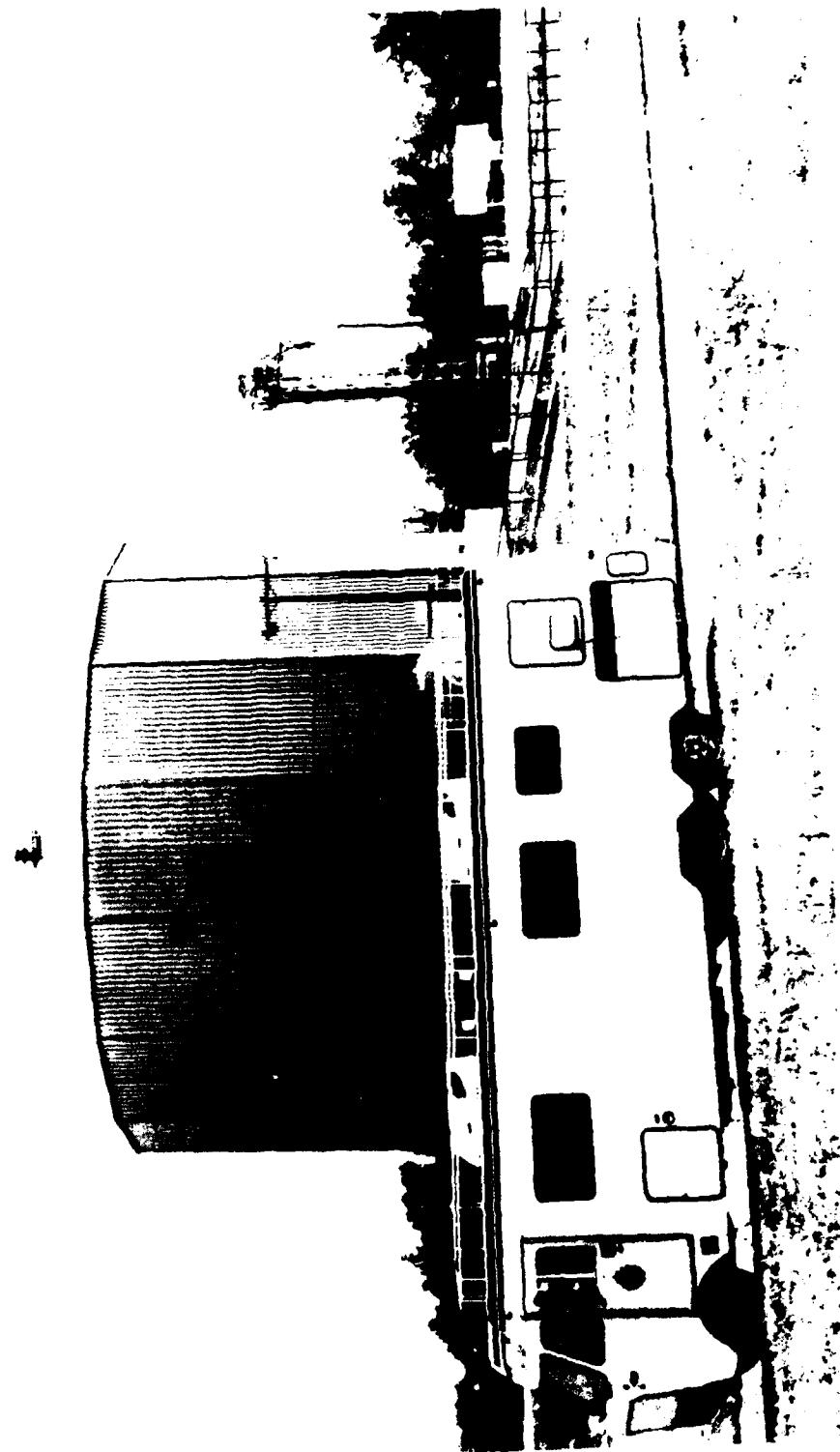
Plate 1 : DREO mobile nuclear laboratory at the APRD reactor facility.

Comparison of Kerma Determinations

Kerma values, either inferred from spectral determinations or measured directly by the three groups, are compared in Table 4. Also listed are kermas predicted by theoretical calculations performed at DREO and the Oak Ridge National Laboratory (ORNL), described in detail in a later section of this report.

Thermal-neutron kerma is defined as that carried by neutrons in thermal equilibrium with their environment. Experimentally this is usually determined using cadmium filters for which the upper cut-off energy is 0.5 electron-volts. The DREO measurements were made using BF3 counters, whereas APRD used gold activation foils. The theoretical calculations correspond to group 37 of the DLC-31 format.

Epithermal neutron kerma is defined as that contribution due to neutrons between 0.5 eV and the NE-213 lower limit of 600 keV (550 keV in the case of APRD). DREO measurements are based on Cd-BF3 data while APRD's derive from proton-recoil gas counter determinations. Theoretical values result from integration of groups 22 to 36 inclusive.

Fast-neutron kerma is measured by all groups spectroscopically, and includes neutrons above the lower-energy threshold of NE-213 scintillators. Theoretical calculations include neutron groups 1 to 21 inclusive.

Total neutron kerma determined by DREO is obtained by the summation of the above-mentioned components, as is the same quantity calculated theoretically. APRD measures total neutron kerma separately by measuring total radiation kerma with a tissue-equivalent ion chamber and subtracting the gamma-ray component determined by a Geiger-Mueller chamber.

Gamma-ray kerma is determined spectroscopically by DREO and WWD using NE-213 detectors (above thresholds of 300 and 450 keV respectively). APRD measurements are based on G-M data as previously mentioned. Theoretical predictions include all gamma-ray groups, namely groups 38 to 58 of the DLC-31 format.

Total radiation kermas are determined by summation of neutron and gamma-ray components, except in the case of APRD, for which ion chamber measurements yield this quantity directly.

At the fifteen-metre experimental position, theoretical values are unavailable due to the previously noted difference in core heights (5.34 metres versus 14 metres). APRD and WWD measurements to 400 metres are reproduced from references 3 and 11. APRD kermas at 1100 metres were recently measured and the results transmitted by private communication (15). The ORNL calculations were similarly obtained, although some details have been reported elsewhere (16). Since the radial limit of the ORNL calculation was 500 metres, no comparisons are presented beyond this distance.

Agreement between DREO and APRD determinations of total neutron, gamma-ray, and total radiation kerma is excellent, especially considering that entirely different techniques were used by each group and that no common calibrations existed previously. APRD detectors had been calibrated at the US National Bureau of Standards (NBS) whereas DREO detector responses were determined theoretically, except in the case of the BF3 counters which were calibrated at the National Research Council of Canada (NRCC). No consistent variations are observed in the data, and in fact the average ratio of individual kerma determinations is calculated to be 1.02, with an r.m.s. variation about this value of 0.10. DREO data are estimated to be accurate to within 5 %, and APRD to within 3 %. Over and above these estimates must be included a reproducibility of 2 % in total reactor power level between runs.

RANGE	QUANTITY	EXPERIMENTAL			THEORETICAL	
		DREO	APRD	WWD	DREO	ORNL
15 metres	Thermal neutron	8.39-20				
	Epithermal neutron	2.99-17				
	Fast neutron	8.50-17				
	Total neutron	1.15-16				
100 metres	Thermal neutron	7.73-21			6.22-21	
	Epithermal neutron	6.36-19			4.35-19	
	Fast neutron	1.35-18	1.63-18	1.72-18	1.27-18	
	Total neutron	2.00-18	2.24-18		1.71-18	2.17-18
	Gamma-ray	3.84-19	3.23-19	3.89-19	3.50-19	4.61-19
	Total Kerma	2.38-18	2.56-18		2.06-18	2.63-18
170 metres	Thermal neutron	2.79-21	2.44-21		2.80-21	
	Epithermal neutron	1.83-19	1.99-19		1.60-19	
	Fast neutron	3.64-19	4.92-19	4.46-19	4.12-19	
	Total neutron	5.49-19	5.53-19		5.75-19	5.51-19
	Gamma-ray	1.32-19	1.25-19	1.34-19	1.10-19	1.39-19
	Total Kerma	6.81-19	6.78-19		6.85-19	6.90-19
300 metres	Thermal neutron	6.63-22			5.78-22	
	Epithermal neutron	2.60-20			2.79-20	
	Fast neutron	5.07-20	7.95-20	6.31-20	6.78-20	
	Total neutron	7.73-20	8.75-20		9.62-20	9.54-20
	Gamma-ray	2.87-20	2.60-20	2.67-20	2.20-20	2.14-20
	Total Kerma	1.06-19	1.14-19		1.18-19	1.17-19
400 metres	Thermal neutron	2.32-22			2.21-22	
	Epithermal neutron	8.78-21			8.82-21	
	Fast neutron	1.65-20			2.04-20	
	Total neutron	2.55-20			2.94-20	3.11-20
	Gamma-ray	1.10-20			8.47-21	1.15-20
	Total Kerma	3.65-20	3.68-20		3.79-20	4.26-20
1100 metres	Thermal neutron	7.05-25			1.77-24	
	Epithermal neutron	3.35-23			3.94-23	
	Fast neutron	5.88-23			7.22-23	
	Total neutron	9.30-23	8.27-23		1.13-22	
	Gamma-ray	8.39-23	1.01-22		9.02-23	
	Total Kerma	1.77-22	1.84-22		2.04-22	

Table 4 : Comparison of kerma values (rads per source neutron) measured by DREO, APRD, WWD and calculated by DREO and ORNL.

Any individual differences between APRD- and DREO-determined estimates of total neutron, gamma-ray, or total radiation kerma are thus without statistical significance considering the expected variation of 10 %.

The component of fast-neutron kerma detected by NE-213 scintillators shows a greater variation amongst the three groups. Typically DREO estimates are the lowest and APRD the highest. This discrepancy is consistent with the variations in neutron spectra previously discussed, and would result from the same cause. Gamma-ray kerma measurements of DREO and WWD (both using NE-213) are, however, within experimental error.

At a range of 170 metres APRD have more complete information as this position is used in addition for other investigations. In particular, measurements of thermal and epithermal neutron kermas have been made, both being in satisfactory agreement with DREO determinations.

Comparison of measured to theoretical kerma values will be made in a later section of this report.

The contributions of each component of kerma measured by DREO are shown as fractions of the total in Figure 9. The solid lines are merely best-fit curves to the measured data and are not theoretically derived. As expected, individual neutron components and total neutron kerma fractions decrease continuously with increasing distance. Gamma-ray kerma increases relative to neutron kerma for two reasons. Gamma rays have a somewhat longer mean-free-path in the atmosphere and are consequently less rapidly attenuated. Secondly, gamma-rays are produced following neutron capture, and these capture gamma rays eventually dominate at sufficiently great distances.

Comparison of Neutron Fluences above 3 MeV

Total neutron fluences above 3 MeV may be measured by integration of NE-213-determined neutron spectra, or by the activation of sulfur pellets. Table 5 summarizes measurements made by DREO, APRD and WWD, and also corresponding theoretical calculations.

LABORATORY	METHOD	100 m	170 m	300 m	400 m	1100 m
DREO	NE-213	8.72-11	2.23-11	3.14-12	9.94-13	3.27-15
WWD	NE-213	8.20-11	2.12-11	2.86-12		
APRD	NE-213	9.35-11	2.69-11	3.79-12		
APRD	2" SULFUR	9.60-11	2.38-11	3.23-12		
APRD	1" SULFUR	8.35-11	2.32-11	3.90-12		
DREO	DOT-3	6.62-11	1.71-11	2.40-12	7.85-13	3.01-15
ORNL	DOT-3	7.32-11	1.67-11	2.65-12		
AVERAGE	EXPT.	8.84-11	2.35-11	3.38-12	9.94-13	3.27-15
AVERAGE	CALC.	6.97-11	1.69-11	2.53-12	7.85-13	3.01-15
RATIO : CALC./EXPT.		0.79	0.72	0.75	0.79	0.92

Table 5 : Neutron fluences above 3 MeV (neutrons per square centimetre and per source neutron) measured and calculated at five distances from the reactor core.
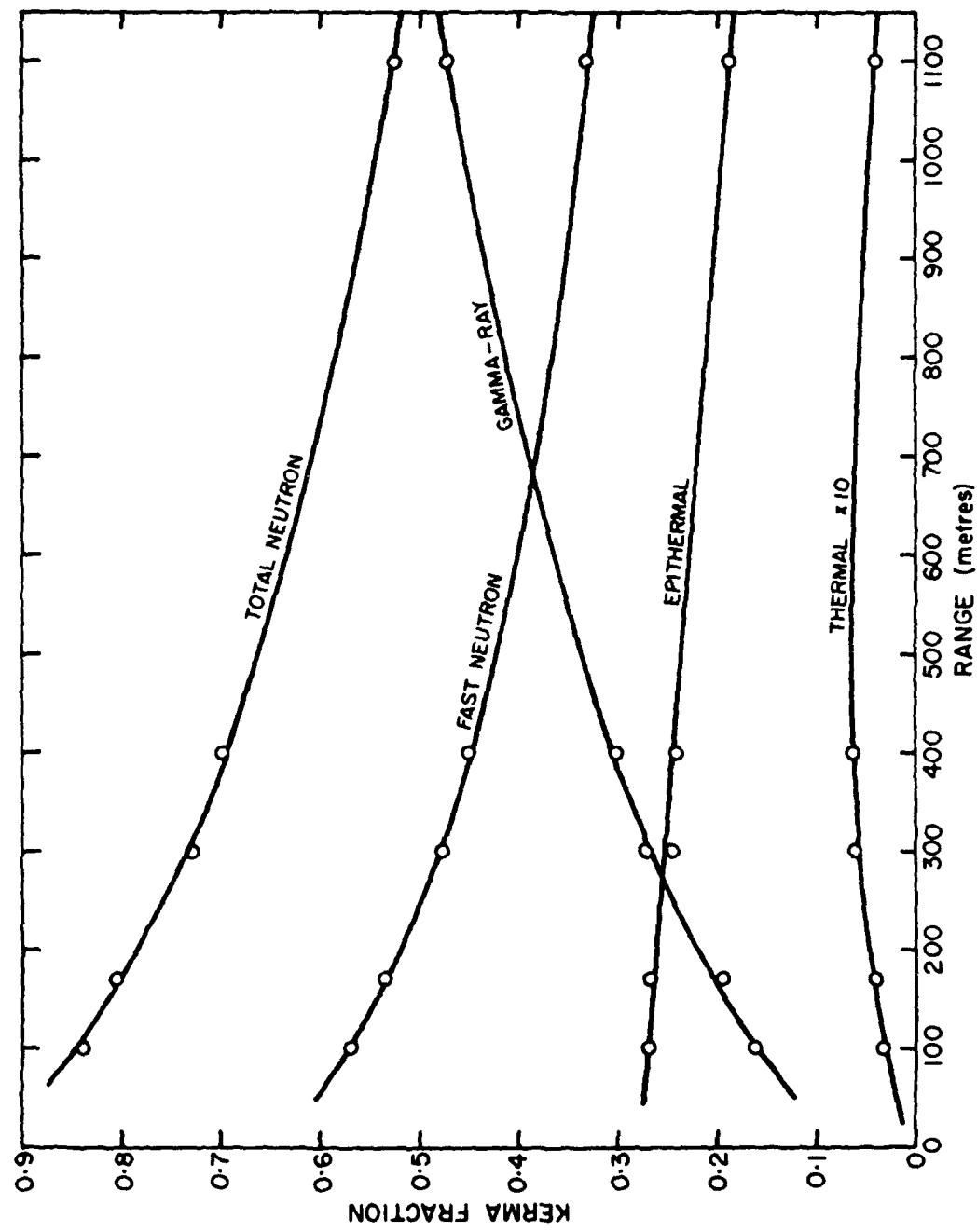
Figure 9 : Contributions to total kerma measured by DREO.

Experimental measurements are consistent to within observed variations of about 10 %, with the sulfur data tending to be on the average somewhat higher than the NE-213 determinations.

THEORETICAL CALCULATIONS

Theoretical calculation of neutron and gamma-ray spectra was made using the DOT-3 two-dimensional discrete-ordinates radiation transport code (17). The calculation covered a space mesh extending to 1600 metres both in altitude and range, and to a depth of 1.65 metres below ground, using 15 radial and 25 axial cell boundaries. Anisotropy of particle scattering and fluence was considered in the P3-S6 (30-angle) approximation. The distribution over particle energy followed the DLC-31 data-library structure of 37 neutron and 21 gamma-ray groups (7). The radiation source was modelled at a height of 14 metres above ground, with neutron and gamma-ray spectra taken from (3), as listed in Appendix I. The source consisted of one neutron and 0.65 photons, and the uncollided fluences arising therefrom were determined using the analytic first-collision option of the DOT-3 code. Neutron and gamma-ray kermas were obtained by integrating the calculated spectra against the DLC-31 fluence-to-kerma conversion factors, also listed in Appendix I.

The compositions of nuclide mixtures used to represent the ground and atmospheric regions are tabulated below.

Element	Density (atoms/barn-cm)	
	Air	Ground
Hydrogen		4.216E-2
Nitrogen	4.024E-5	
Oxygen	1.070E-5	5.917E-2
Sodium		2.600E-4
Aluminum		1.300E-3
Silicon		1.904E-2
Iron		3.500E-4
Density :	$1.22E-3 \ g/cm^3$	$2.632 \ g/cm^3$

Table 6 : Elemental compositions and densities of air and ground.

The nitrogen and oxygen cross-section sets chosen were those resulting from fission-weapon spectral weighting (as opposed to 1/E weighting) of the original data preparation by ORNL (7). The composition of the ground mixture was selected to be consistent with the average of "dry soil" and "wet soil" analyses performed by APRD (3).

Discrete-ordinates calculations involving point sources in two-dimensional geometries often exhibit a numerical artifact known as discrete ray-streaming. Briefly, this results from radiation streaming preferentially away from the source along the discrete directions defined by the angular quadrature. To determine the extent of this effect on the present calculations, Figures 10 to

20

APRF REACTOR - SOURCE = 1 NEUTRON + 0.65 PHOTONS

NEUTRON KERMA (rads/source neutron)

ALTITUDE (m)

1500

0

-1.50

1500

GROUND RANGE (m)

10^{-18}
10^{-19}
10^{-20}
10^{-21}
10^{-22}
10^{-23}

1500

0

-1.50
1500

ALTITUDE (m)
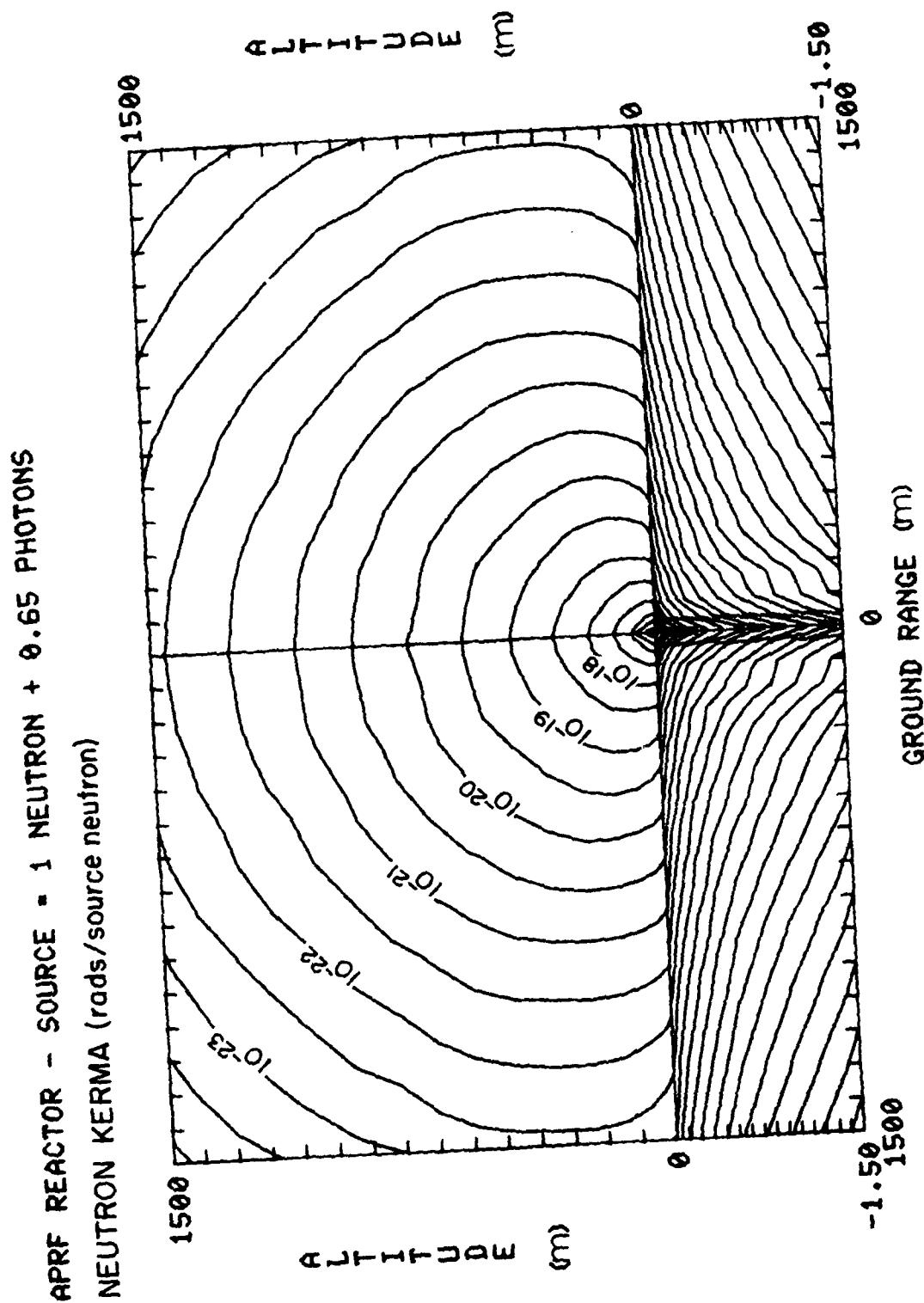
Figure 13 : Contours of total neutron kerma over the theoretical space mesh.
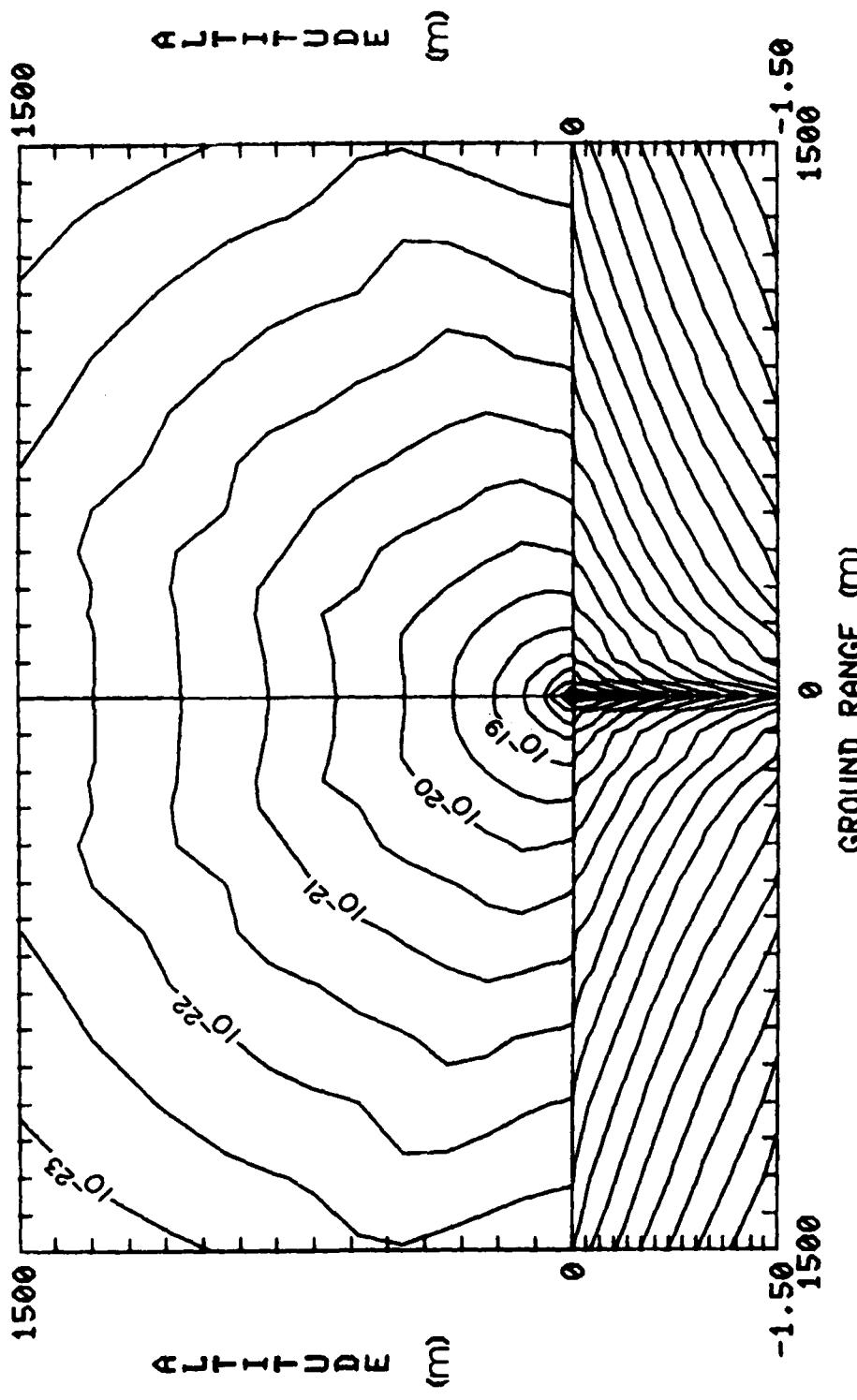
Figure 11 : Contours of total gamma-ray kerma over the theoretical space mesh.

22
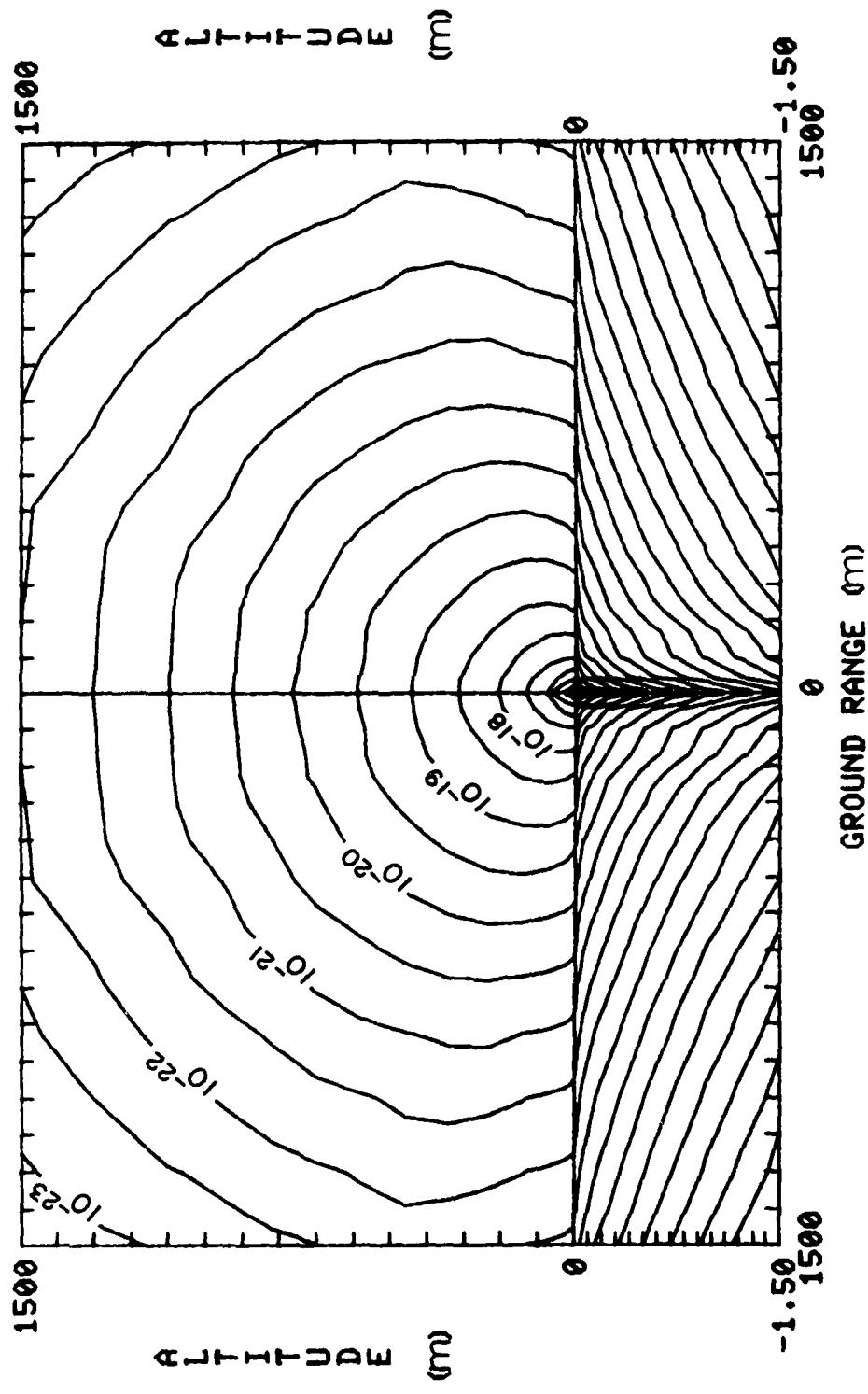
Figure 12 : Contours of total radiation kerma over the theoretical space mesh.

12 were prepared showing the spatial contours of neutron, gamma-ray, and total radiation kermas over the theoretical space mesh. Note that in each plot the vertical scale below the air/ground interface has been greatly expanded, thus causing the distortion apparent immediately below the radiation source. The smoothness of the contours of Figure 10 indicates that the calculation of neutron kerma has not been seriously affected. It is interesting to note the influence of the ground as primarily an absorber, in that the contour lines are "pulled in" towards the source near the interface, thus causing individual contours to propagate farther vertically than horizontally (i.e. depart from a semi-circular shape).

Contours of gamma-ray kerma (Figure 11) appear to be much more affected by ray-streaming, apparent at directions of about 20 degrees to both the vertical and horizontal axes. Near the the air/ground interface this effect does not, however, appear to be very severe and thus should not be a source of significant error for the purposes of comparison to experimental measurement. The total kerma contours of Figure 12 are influenced similarly, but only to the extent that gamma rays contribute to the total kerma.

The Oak Ridge calculations referred to previously were also performed using the DOT-3 code (P3-S8 approximation), employing a similar air density of 1.228 grams/litre but with a hydrogen soil content 28 % greater (0.054 atoms per barn-cm). The ORNL calculations were, however, made only out to a maximum ground range of 500 metres.

COMPARISON OF CALCULATED AND MEASURED DATA

Neutron Spectra

In Figures 13 to 17 comparisons are made of DREO measured and calculated neutron spectra at the five ground ranges between 100 and 1100 metres. Normalization in each case is made to a single source neutron. At a range of 100 metres there is a consistent underprediction by the calculations of about 25 %, except below 2 MeV where the agreement is much better. At ranges of 170, 300 and 400 metres there is similar underprediction by theory above 3 MeV, but compensating overprediction below 2 MeV. The best overall agreement occurs at the farthest range of 1100 metres, being almost faultless above 2 MeV, but with significant overprediction below 1 MeV. The improvement in agreement with increasing ground range is somewhat surprising - usually the opposite behaviour is observed in typical radiation transport experiments. It might be suspected that the presence of the hill at the 1100 metre position is responsible. It is the authors' opinion, however, that this is not the case since any elevation of the detector above the primary ground plane should result in an increase of experimental measurement with respect to calculation. In fact the opposite is observed, namely the measured spectrum is reduced relative to that predicted by the DOT code, in comparison to the difference noted at the other measurement positions. It is therefore concluded that the perturbation caused by the hill is insignificant to the present study, and that the ground beneath the detector influences the local radiation environment to a similar extent as at the other measurement positions.
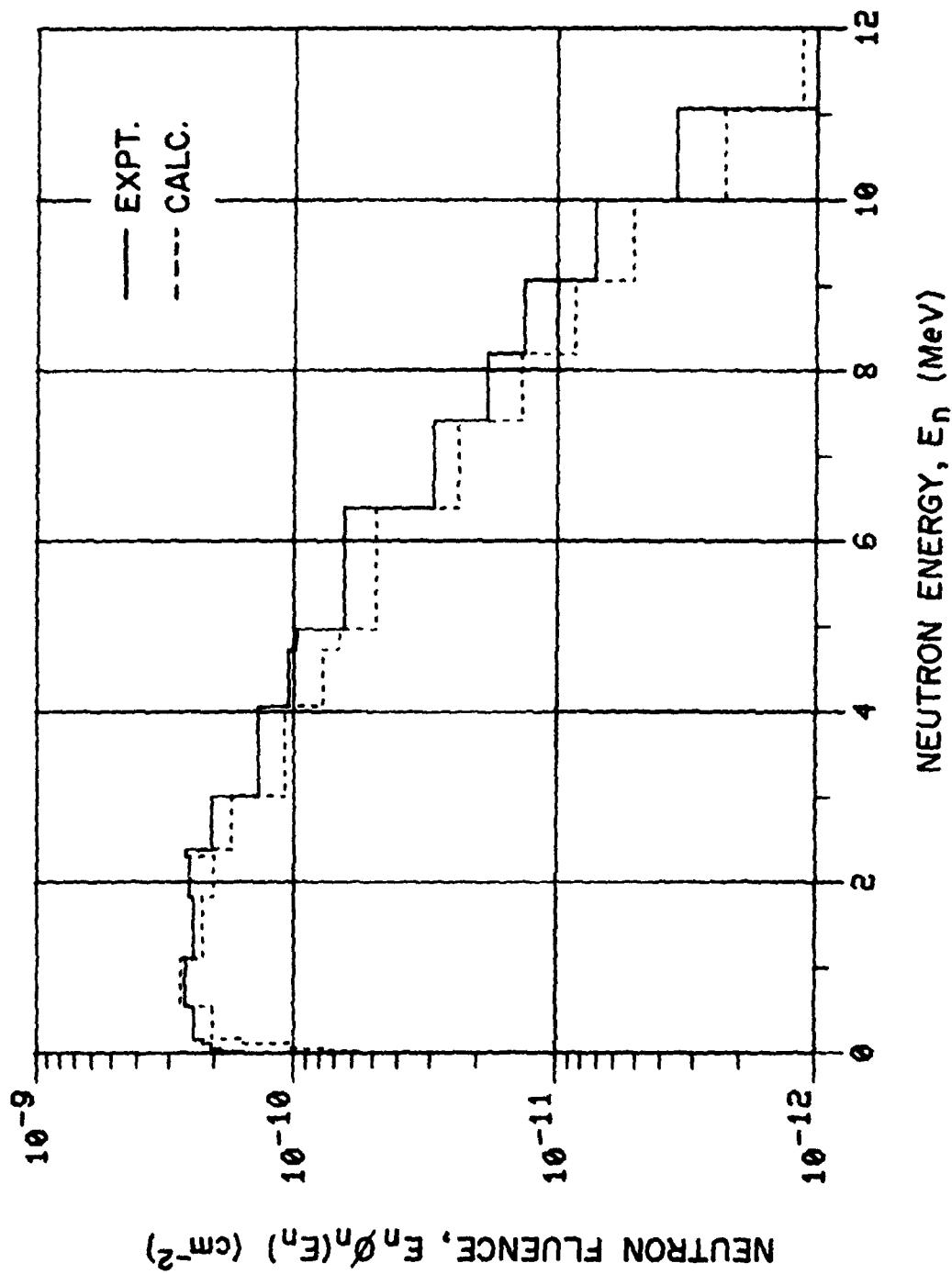
Figure 13 : DREO measured and calculated neutron spectra at a ground range of 100 metres.
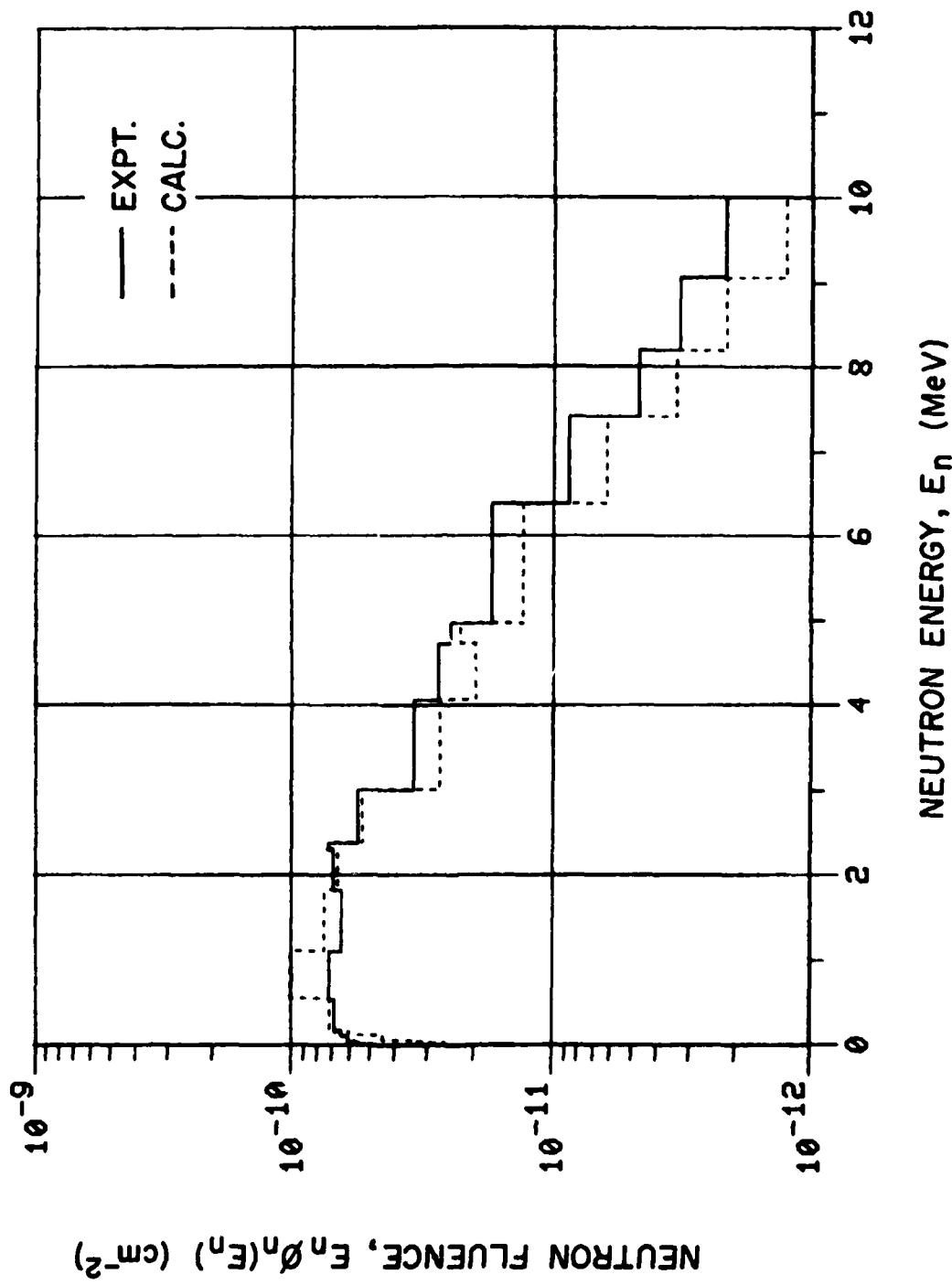
Figure 14 : DREO measured and calculated neutron spectra at a ground range of 170 metres.

NEUTRON ENERGY, E_n (MeV)
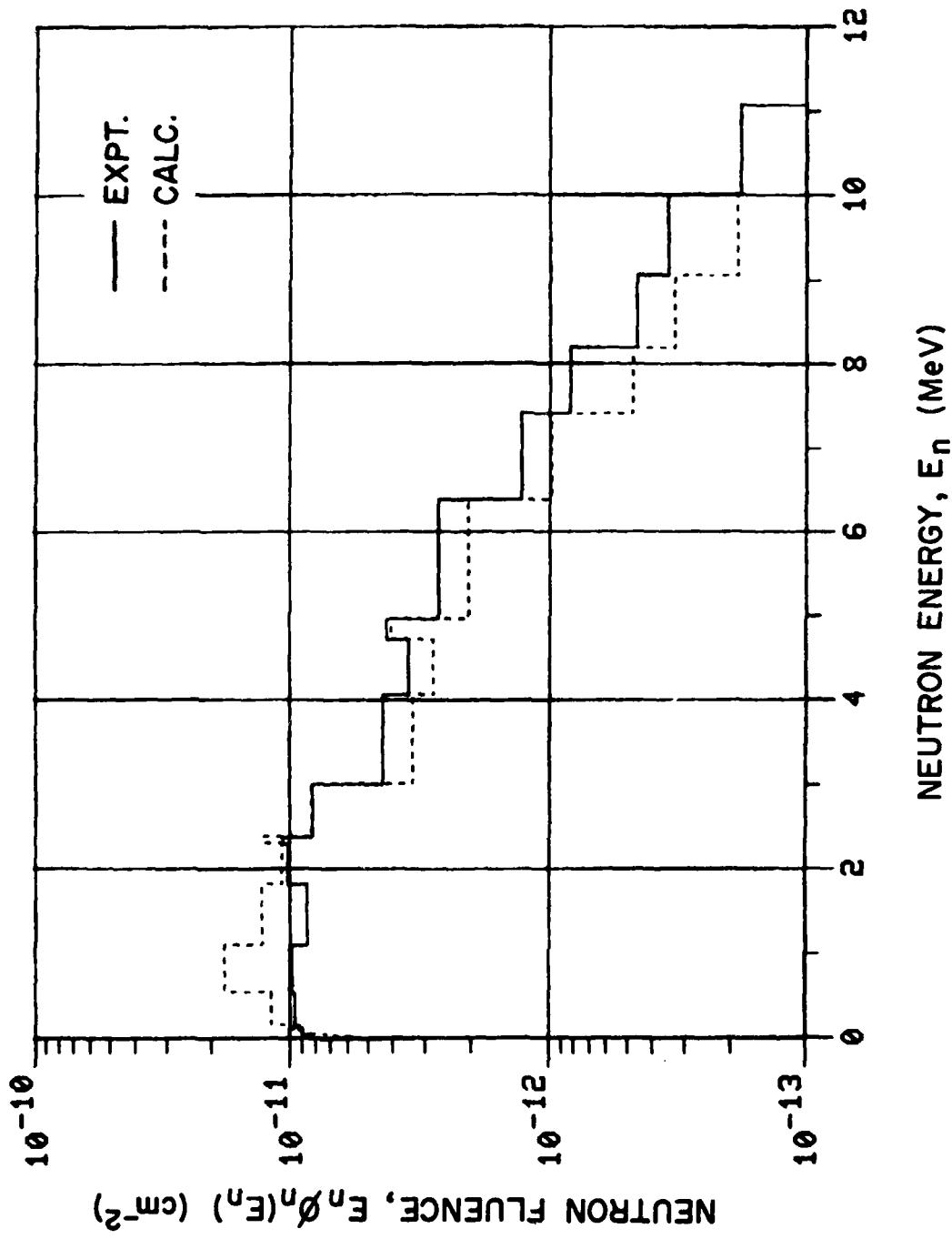
Figure 15 : DREO measured and calculated neutron spectra at a ground range of 300 metres.
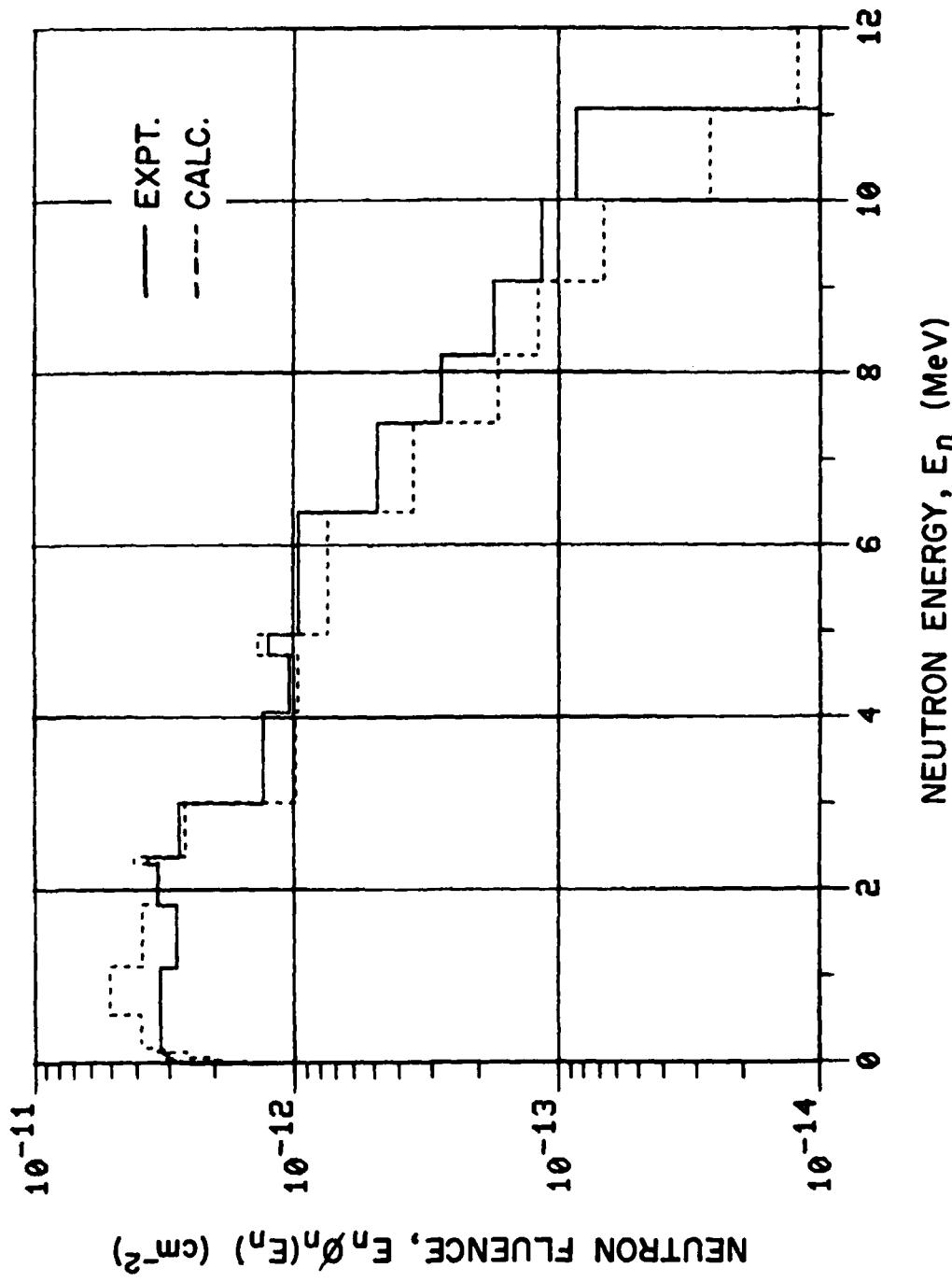
Figure 16 : DREO measured and calculated neutron spectra at a ground range of 400 metres.

28
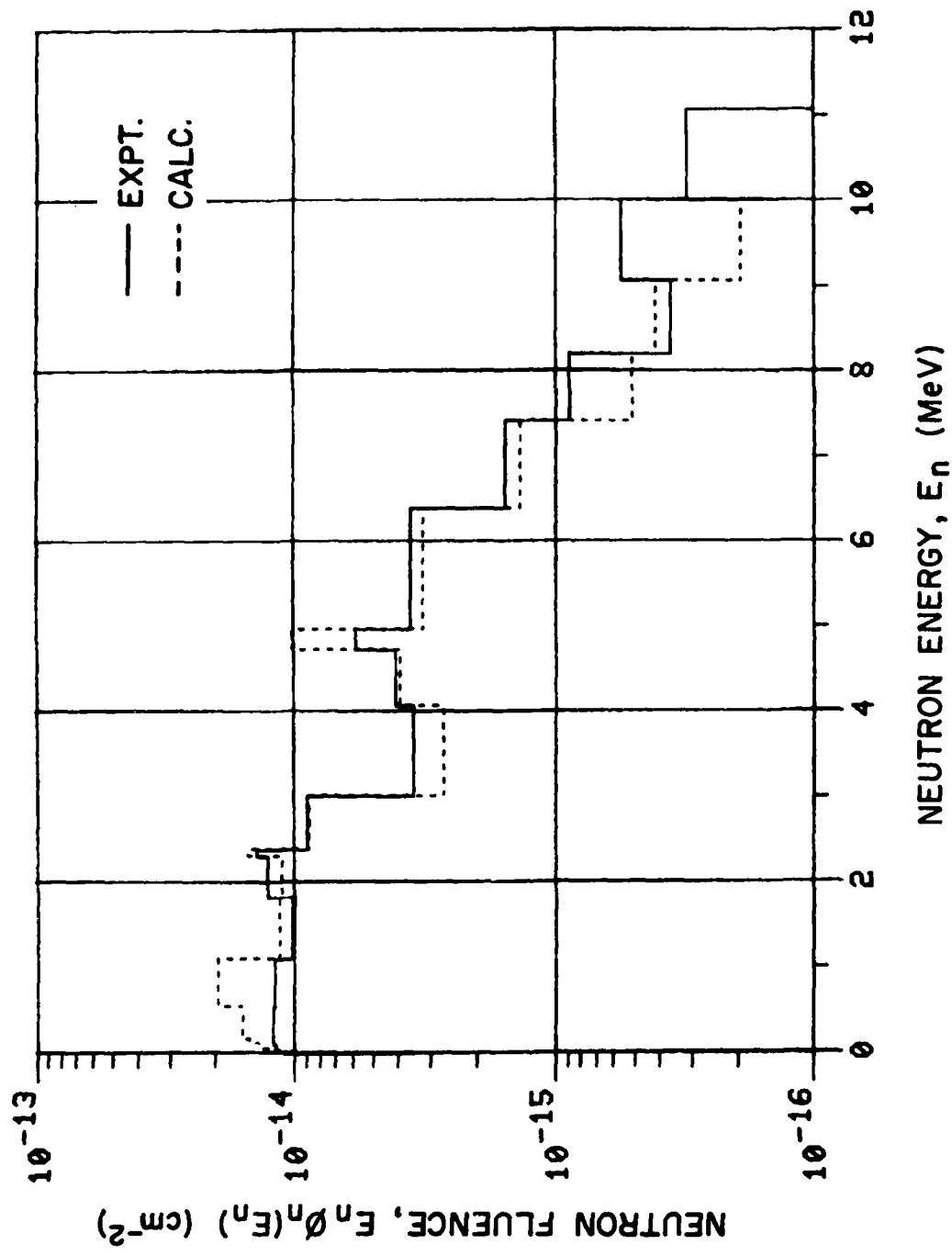
Figure 17 : DREO measured and calculated neutron spectra at a ground range of 1100 metres.

Two additional comparisons are made in Figures 18 and 19 of neutron spectra at the 170 metre measurement position. Figure 18 was adopted from (16), comparing APRD measurements with ORNL calculations. Figure 19 is plotted in a similar log-log fashion showing the corresponding DREO measured and calculated neutron spectra. The DREO and ORNL calculated spectra agree essentially exactly, and the APRD measured spectrum is at variance with theoretical prediction to a similar extent as the DREO measurement.

Gamma-ray Spectra

Comparisons of DREO measured and calculated gamma-ray spectra are shown in Figures 20 to 24. Consistent underprediction by theory is apparent at photon energies in excess of 2.5 MeV, for the four measurement positions to 400 metres. It should be noted that the measured data of WWD (Figues 6 to 8) are in somewhat better agreement with theoretical predictions than are the DREO data, however the same discrepancy is apparent above 2.5 MeV, but to a lesser extent. At the 1100-metre position the agreement is almost exact between DREO measurements and calculations. As was the case with neutron spectra, the agreement of gamma-ray spectra is best at the farthest distance from the reactor core.

Integral Quantities

Referring back to Table 4 (page 16), it is apparent that neutron, gamma-ray, and total radiation kermas, both measured and calculated, are in satisfactory agreement. ORNL and DREO theoretical estimates agree generally to within 10 % - in many cases agreement is nearly perfect. Measured and calculated DREO estimates of these three quantities do not appear to be significantly different, as Figure 25 indicates. The estimated experimental error of the DREO data of 7 % is represented by the diameter of the plotted points. As previously noted, the experimental measurements of APRD, WWD and DREO are also in good agreement.

Total neutron fluences above 3 MeV are underpredicted by theoretical calculation (Table 5, page 17) by approximately 25 % at the first four measurement locations. At the 1100-metre position the difference is reduced to only 8 %. These differences are consistent with those of the previously discussed neutron spectra.

30
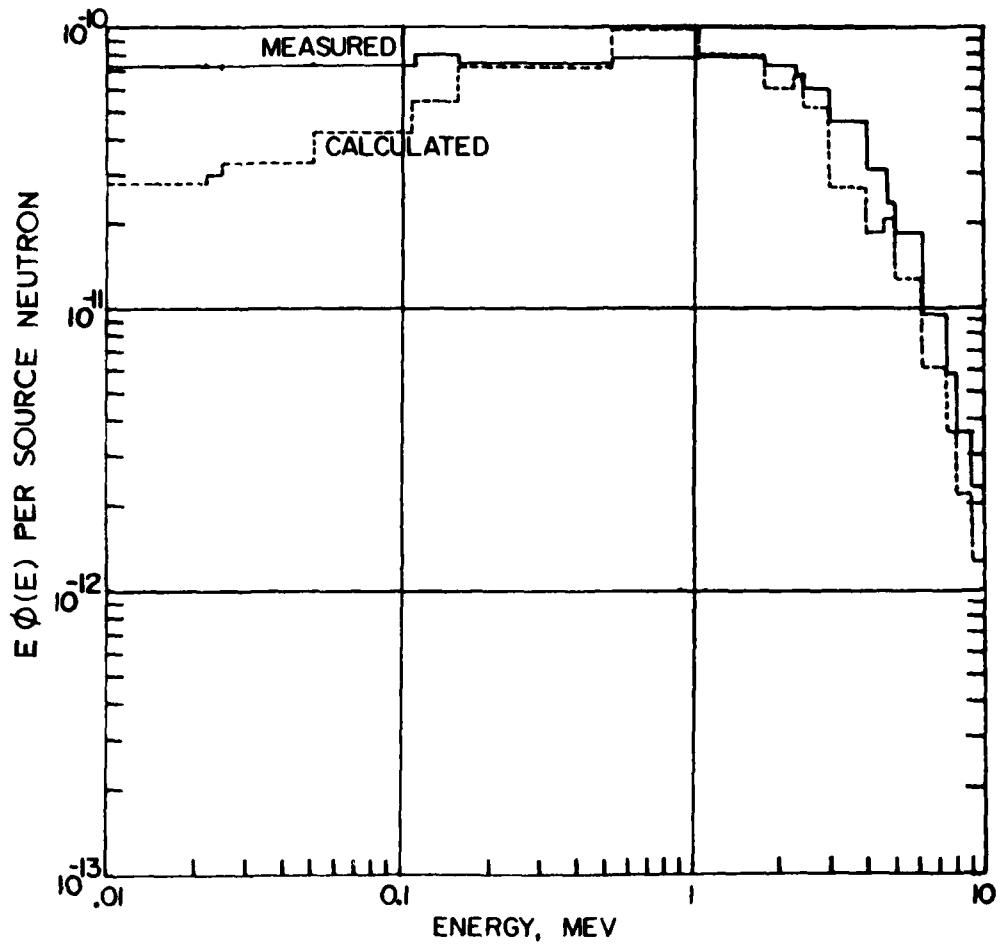
Figure 18 : APRD measured and ORNL calculated neutron spectra
at a ground range of 170 metres.
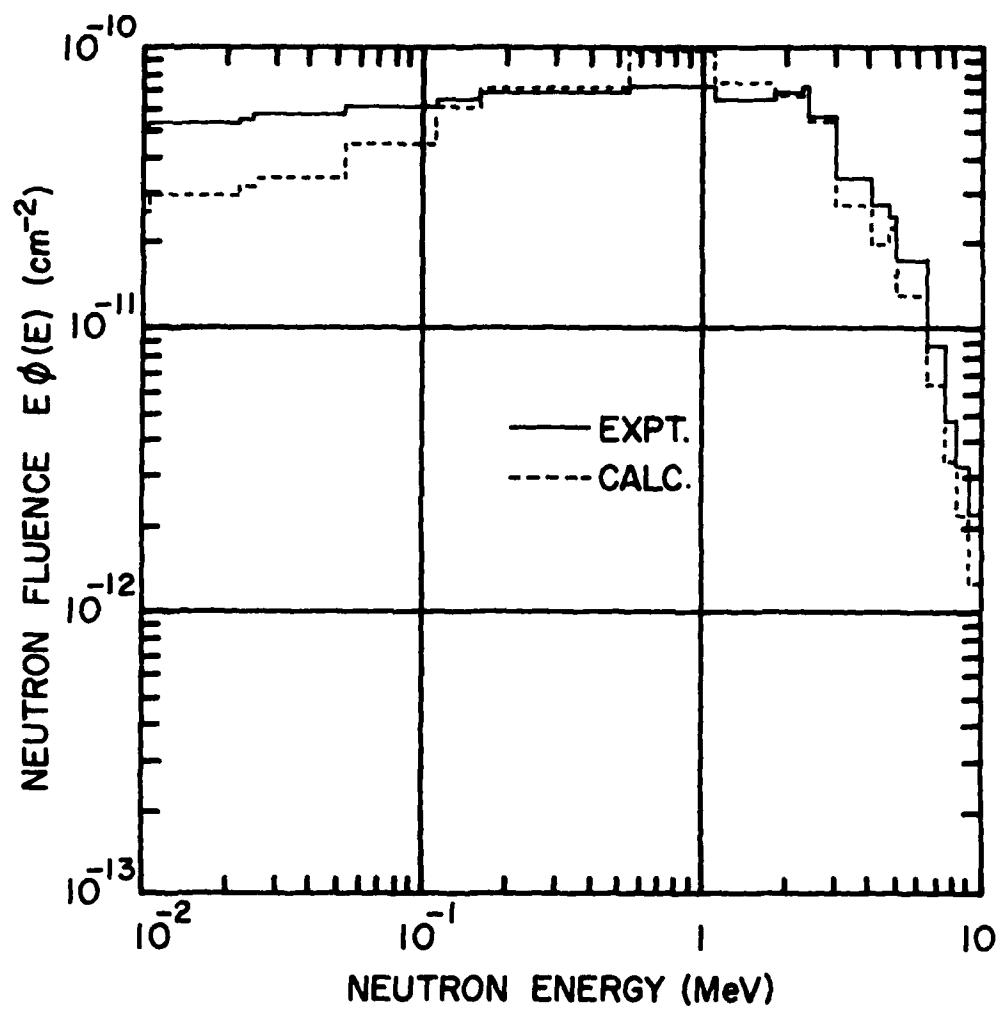
Figure 19 : DREO measured and calculated neutron spectra at a
ground range of 170 metres.
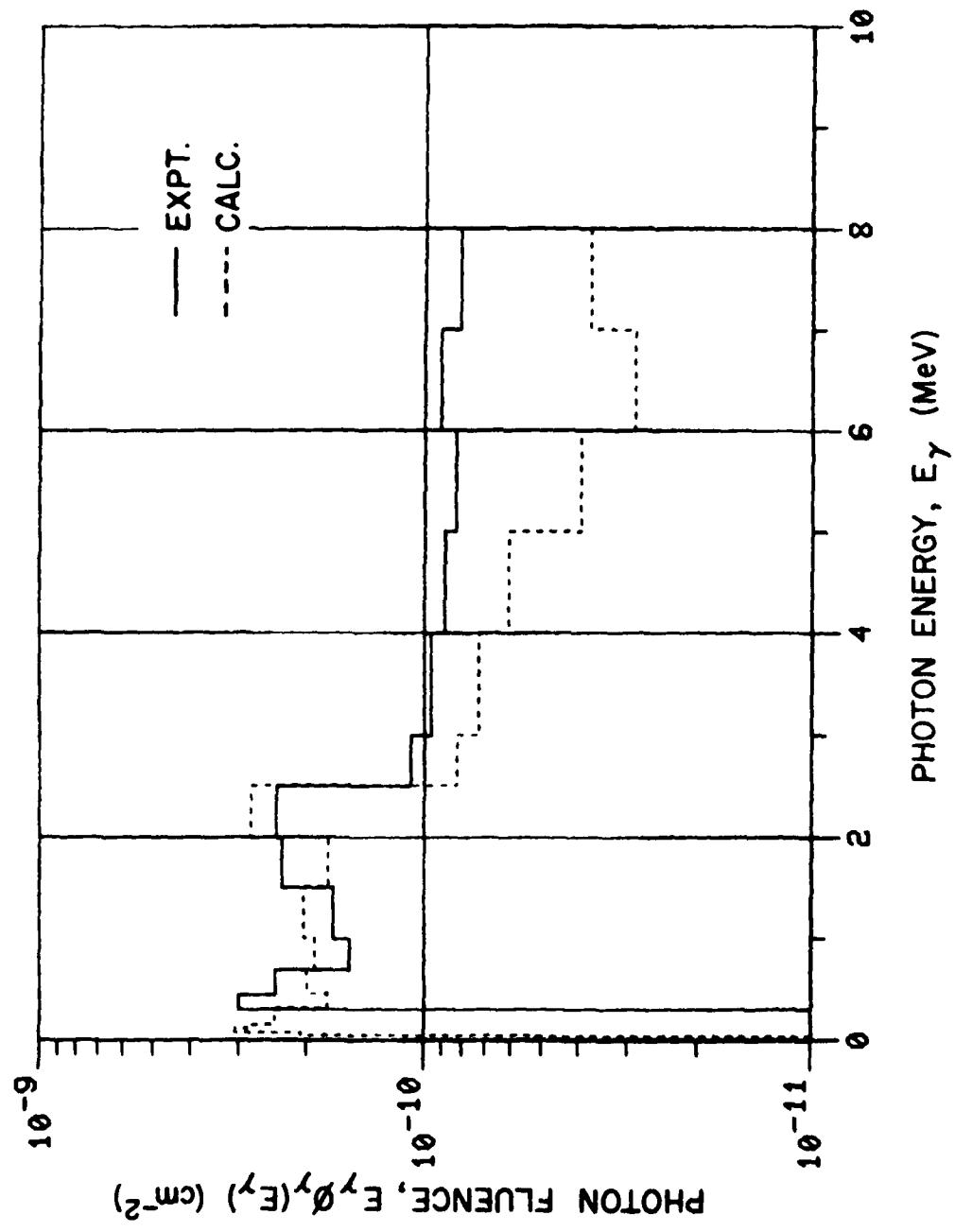
PHOTON ENERGY, E_γ (MeV)

PHOTON FLUENCE, $E_\gamma \phi_\gamma(E_\gamma)$ (cm^{-2})

Figure 20 : DREO measured and calculated gamma-ray spectra at a ground range of 100 metres.
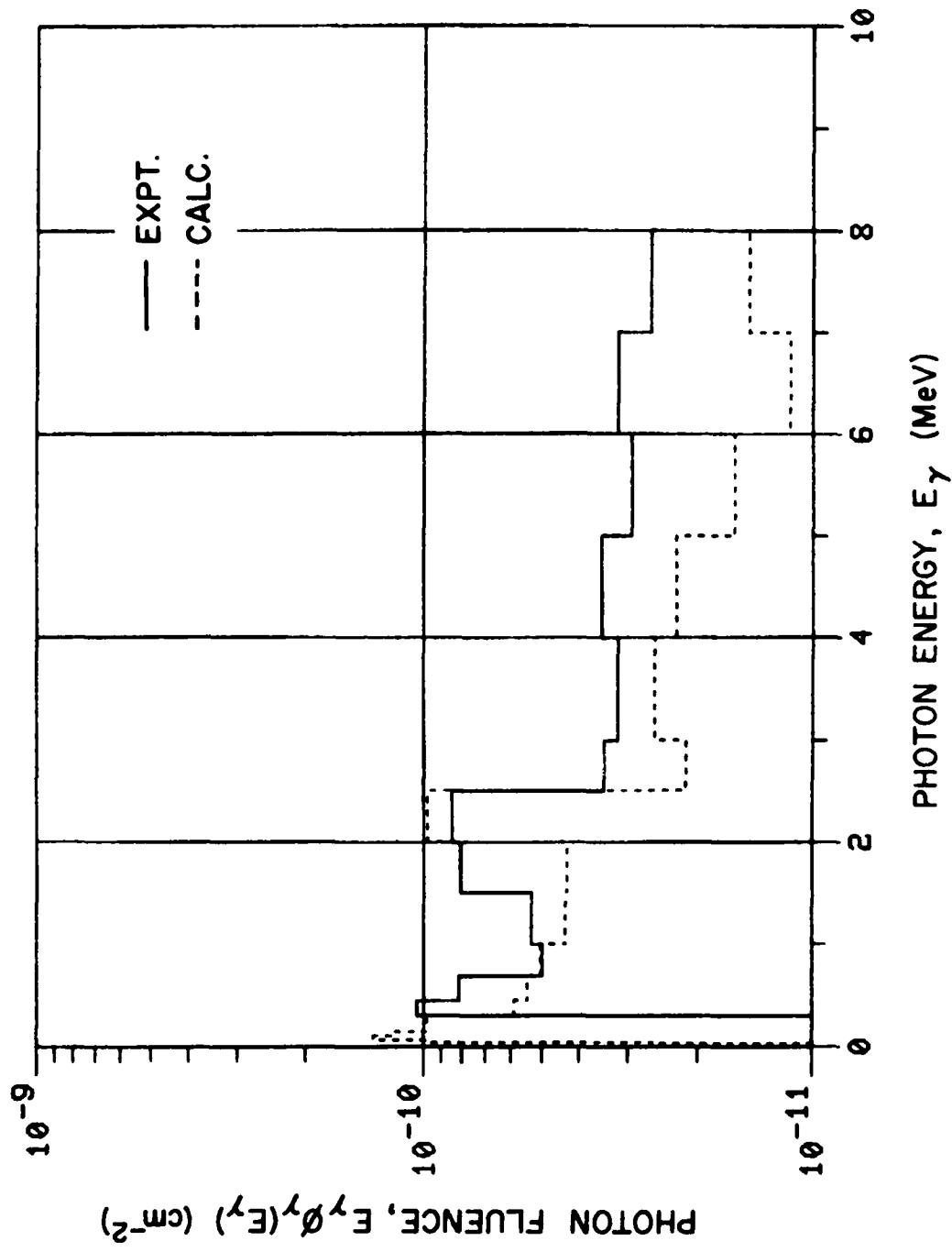
Figure 21 : DREO measured and calculated gamma-ray spectra at a ground range of 170 metres.
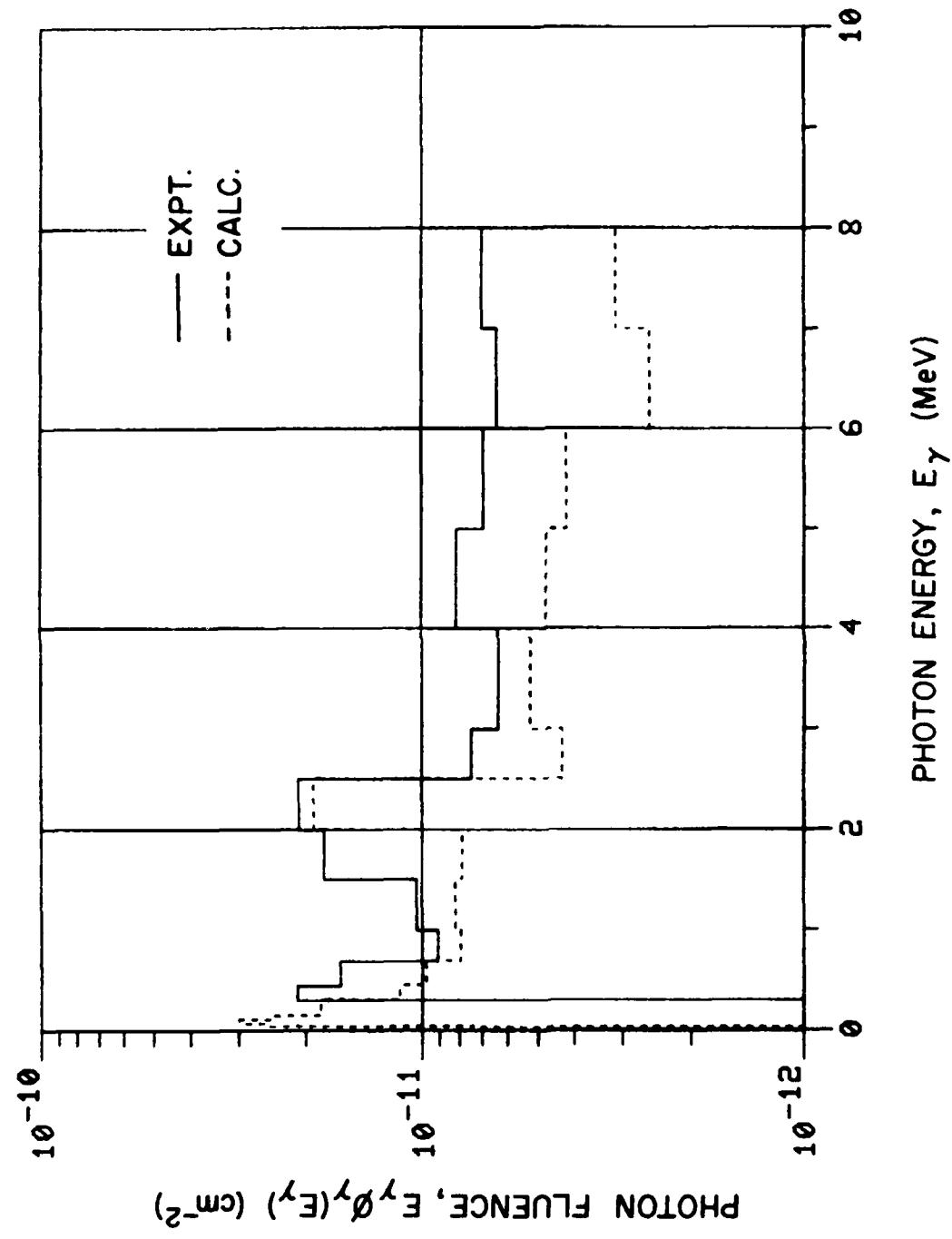
Figure 22 : DREO measured and calculated gamma-ray spectra at a ground range of 300 metres.

Figure 23 : DREO measured and calculated gamma-ray spectra at a ground range of 400 metres.

PHOTON ENERGY, E_γ (MeV)

PHOTON FLUENCE, $E_\gamma \phi_\gamma(E_\gamma)$ (cm^{-2})
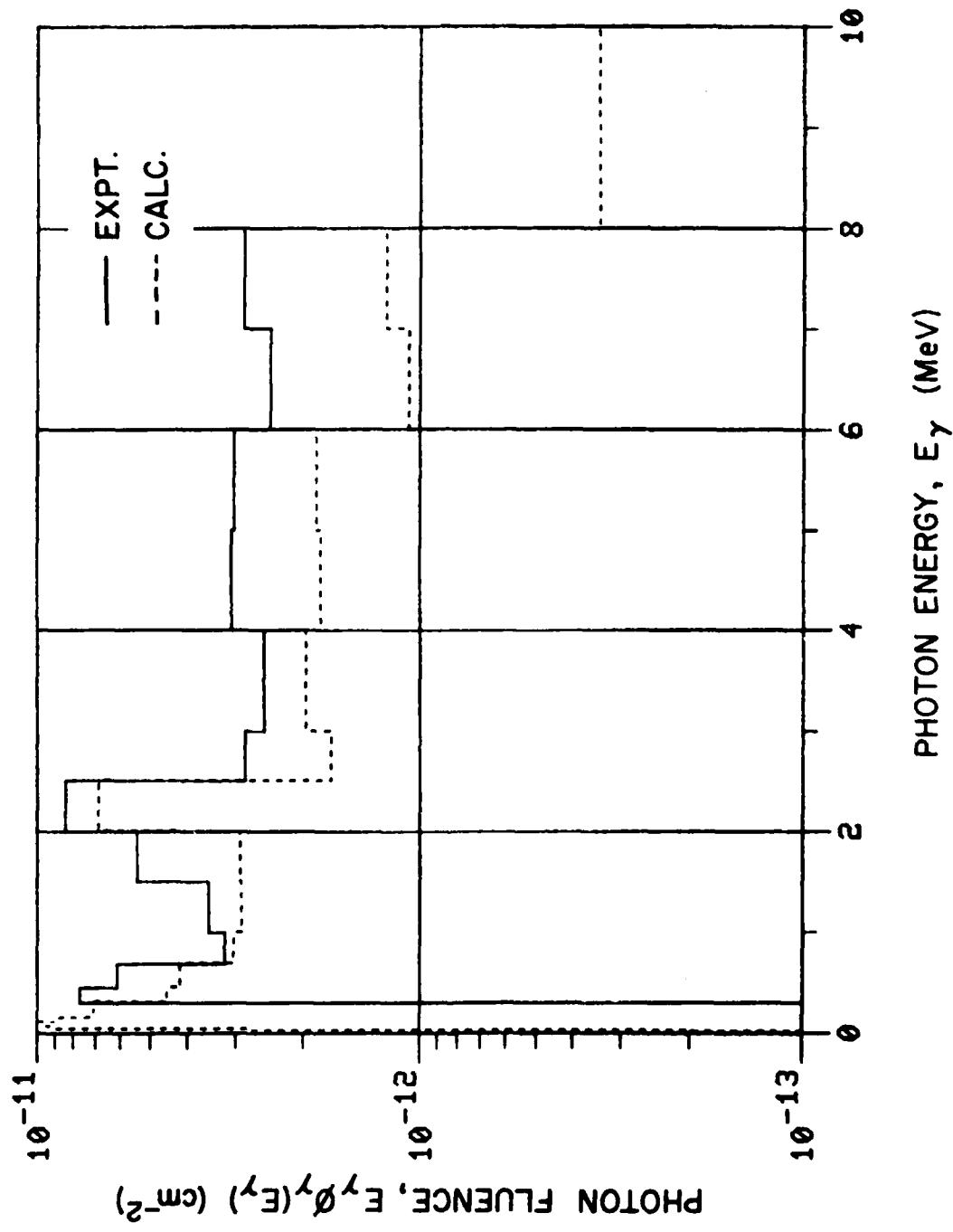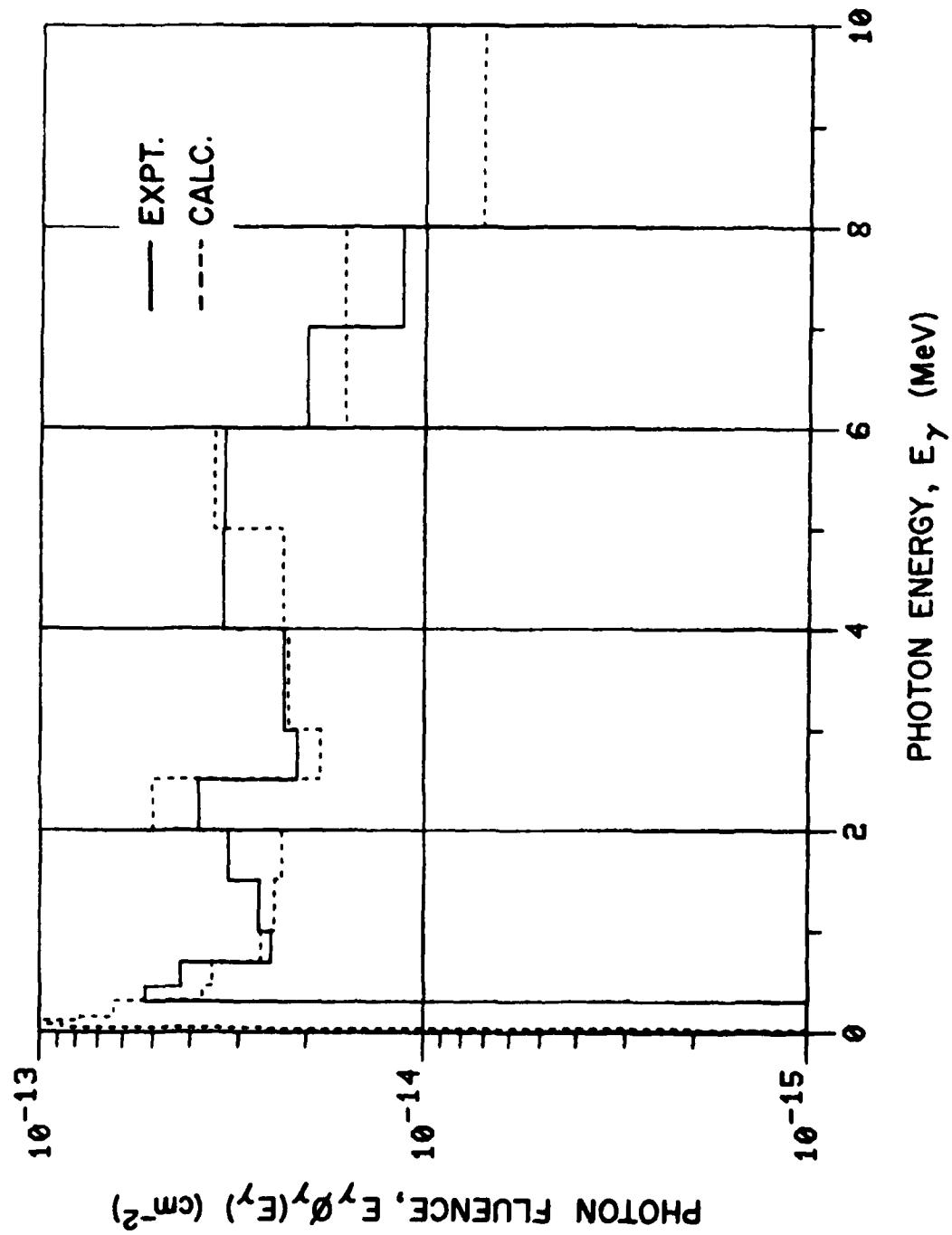
Figure 24 : DREO measured and calculated gamma-ray spectra at a ground range of 1100 metres.
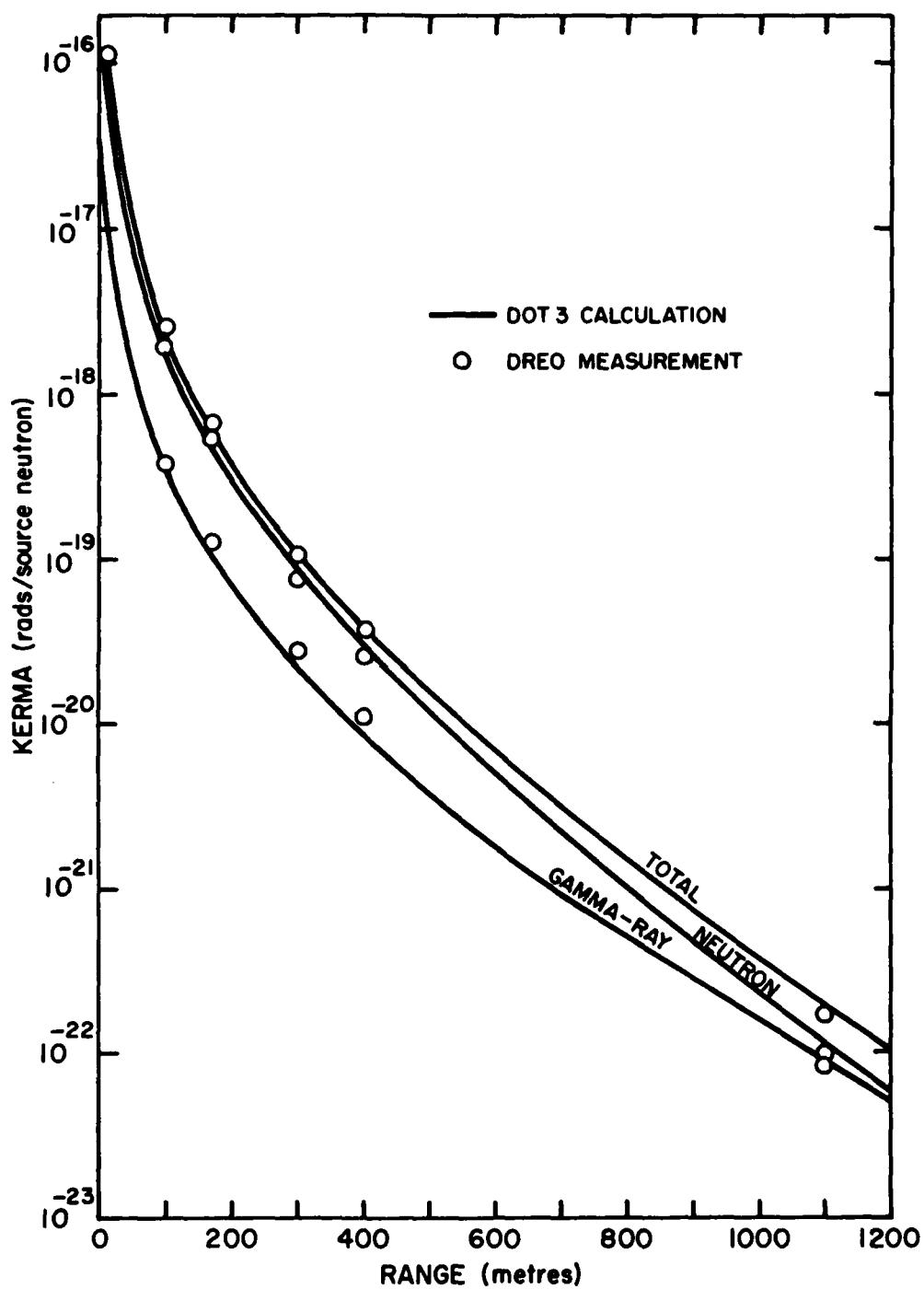
Figure 25 : DREO measured and calculated neutron, gamma-ray
and total radiation kermas.

CONCLUSIONS

The DOT-3 radiation transport code has been shown to accurately predict neutron and gamma-ray kermas within experimental limitation, characteristic of fission sources in an air-over-ground geometry. Particle spectroscopy indicates that calculated spectra are somewhat softer than observed experimentally. The spectral discrepancy is least severe at the farthest measurement distance of 1100 metres. This behaviour is gratifying in that at similar ranges from tactical nuclear weapons nuclear radiation represents the greatest hazard to military personnel, the effects of blast and thermal radiation being less far-reaching.

Although speculative at this stage, improvement in agreement with experimental observation might be achieved by theoretical calculations employing more-finely-subdivided energy discretization.

ACKNOWLEDGEMENT

APPENDIX I : Energy group boundaries (DLC-31 structure), reactor source spectra, and fluence-to-kerma conversion factors for neutrons (groups 1-37) and gamma-rays (groups 38 to 58).

Group	Energy Boundaries (MeV) Lower	Upper	Source (per src neut)	Kerma Factor (rad - cm2)
1	1.690E 01	1.964E 01	.000E 00	6.995E-09
2	1.492E 01	1.690E 01	1.000E-05	6.640E-09
3	1.419E 01	1.492E 01	2.000E-05	6.431E-09
4	1.384E 01	1.419E 01	2.000E-05	6.327E-09
5	1.284E 01	1.384E 01	6.000E-05	6.186E-09
6	1.221E 01	1.284E 01	7.000E-05	6.003E-09
7	1.105E 01	1.221E 01	2.300E-04	5.935E-09
8	1.000E 01	1.105E 01	4.500E-04	5.682E-09
9	9.048E 00	1.000E 01	9.800E-04	5.528E-09
10	8.187E 00	9.048E 00	1.590E-03	5.221E-09
11	7.408E 00	8.187E 00	2.630E-03	5.123E-09
12	6.376E 00	7.408E 00	6.190E-03	4.864E-09
13	4.965E 00	6.376E 00	2.059E-02	4.560E-09
14	4.724E 00	4.965E 00	5.470E-03	4.320E-09
15	4.066E 00	4.724E 00	2.068E-02	4.255E-09
16	3.012E 00	4.066E 00	5.892E-02	4.044E-09
17	2.385E 00	3.012E 00	6.184E-02	3.429E-09
18	2.307E 00	2.385E 00	1.058E-02	3.140E-09
19	1.827E 00	2.307E 00	7.637E-02	3.071E-09
20	1.108E 00	1.827E 00	1.750E-01	2.646E-09
21	5.502E-01	1.108E 00	2.376E-01	2.009E-09
22	1.576E-01	5.502E-01	2.581E-01	1.247E-09
23	1.111E-01	1.576E-01	2.460E-02	7.683E-10
24	5.248E-02	1.111E-01	2.483E-02	5.352E-10
25	2.479E-02	5.248E-02	8.910E-03	3.016E-10
26	2.188E-02	2.479E-02	6.700E-04	2.052E-10
27	1.033E-02	2.188E-02	2.540E-03	1.410E-10
28	3.355E-03	1.033E-02	8.900E-04	6.007E-11
29	1.234E-03	3.355E-03	1.600E-04	2.122E-11
30	5.829E-04	1.234E-03	3.000E-05	8.884E-12
31	1.013E-04	5.829E-04	1.000E-05	3.074E-12
32	2.902E-05	1.013E-04	.000E 00	1.141E-12
33	1.068E-05	2.902E-05	.000E 00	1.124E-12
34	3.059E-06	1.068E-05	.000E 00	1.686E-12
35	1.125E-06	3.059E-06	.000E 00	2.822E-12
36	4.140E-07	1.125E-06	.000E 00	4.599E-12
37	1.000E-11	4.140E-07	.000E 00	1.883E-11
38	1.000E 01	1.400E 01	3.000E-04	3.043E-09
39	8.000E 00	1.000E 01	2.300E-03	2.407E-09
40	7.000E 00	8.000E 00	2.200E-03	2.085E-09
41	6.000E 00	7.000E 00	2.300E-03	1.879E-09
42	5.000E 00	6.000E 00	4.900E-03	1.674E-09
43	4.000E 00	5.000E 00	1.010E-02	1.460E-09
44	3.000E 00	4.000E 00	2.050E-02	1.232E-09
45	2.500E 00	3.000E 00	2.330E-02	1.048E-09
46	2.000E 00	2.500E 00	3.920E-02	9.149E-10
47	1.500E 00	2.000E 00	7.660E-02	7.677E-10
48	1.000E 00	1.500E 00	1.345E-01	5.976E-10
49	7.000E-01	1.000E 00	1.177E-01	4.362E-10
50	4.500E-01	7.000E-01	1.121E-01	3.050E-10
51	3.000E-01	4.500E-01	6.160E-02	1.978E-10
52	1.500E-01	3.000E-01	3.700E-02	1.113E-10
53	1.000E-01	1.500E-01	4.700E-03	5.560E-11
54	7.000E-02	1.000E-01	1.000E-03	4.020E-11
55	4.500E-02	7.000E-02	1.000E-04	4.089E-11
56	3.000E-02	4.500E-02	.000E 00	7.342E-11
57	2.000E-02	3.000E-02	.000E 00	1.633E-10
58	1.000E-02	2.000E-02	.000E 00	5.222E-10

APPENDIX II : DREO-measured neutron and gamma-ray multi-group spectra (units of particles per square-centimetre per group) in the DLC-31 data library structure, at the six measurement positions.

Group	15 m	100 m	170 m	300 m	400 m	1100 m
1						
2						
3						
4						
5						
6						
7						
8	2.8305E-11	3.4838E-13	8.6475E-14	1.8261E-14	8.4996E-15	3.1482E-17
9	6.0121E-11	7.1144E-13	2.1929E-13	3.4953E-14	1.1479E-14	5.5554E-17
10	8.2983E-11	1.3244E-12	3.2681E-13	4.6074E-14	1.7346E-14	3.6175E-17
11	1.5800E-10	1.8339E-12	4.6950E-13	8.2794E-14	2.7654E-14	8.8060E-17
12	3.1108E-10	4.4111E-12	1.2986E-12	1.9060E-13	7.2055E-14	2.3342E-16
13	1.0439E-09	1.5975E-11	4.2614E-12	6.6619E-13	2.3614E-13	8.9029E-16
14	3.2581E-10	4.8405E-12	1.2166E-12	2.0886E-13	6.1466E-14	2.8512E-16
15	1.1325E-09	1.5697E-11	4.0710E-12	5.1913E-13	1.5464E-13	6.0965E-16
16	2.9465E-09	4.0949E-11	1.0103E-11	1.3048E-12	3.8924E-13	1.0376E-15
17	2.9711E-09	4.7551E-11	1.2961E-11	1.8942E-12	6.2990E-13	2.0630E-15
18	5.1056E-10	8.5972E-12	2.3930E-12	3.5494E-13	1.1863E-13	4.5975E-16
19	3.4421E-09	5.8160E-11	1.5975E-11	2.3657E-12	7.6770E-13	2.9161E-15
20	7.4068E-09	1.1970E-10	3.2038E-11	4.2756E-12	1.3749E-12	5.0392E-15
21	1.0124E-08	1.8109E-10	5.0054E-11	6.7778E-12	2.2380E-12	8.2786E-15
22	1.4855E-08	2.9995E-10	8.5039E-11	1.1888E-11	3.9816E-12	1.4990E-14
23	3.4836E-09	7.7463E-11	2.2438E-11	3.2127E-12	1.0879E-12	4.1603E-15
24	6.5104E-09	1.5434E-10	4.5358E-11	6.6006E-12	2.2518E-12	8.7040E-15
25	5.4841E-09	1.4197E-10	4.2560E-11	6.3324E-12	2.1823E-12	8.5595E-15
26	8.2094E-10	2.2394E-11	6.7918E-12	1.0239E-12	3.5495E-13	1.4042E-15
27	4.5044E-09	1.2926E-10	3.9657E-11	6.0559E-12	2.1120E-12	8.4260E-15
28	5.4068E-09	1.7305E-10	5.4418E-11	8.5433E-12	3.0174E-12	1.2260E-14
29	3.7165E-09	1.3471E-10	4.3562E-11	7.0564E-12	2.5282E-12	1.0485E-14
30	2.3617E-09	9.4959E-11	3.1430E-11	5.2255E-12	1.8946E-12	7.9931E-15
31	4.0416E-09	1.8761E-10	6.4161E-11	1.1067E-11	4.0812E-12	1.7642E-14
32	2.0340E-09	1.1288E-10	4.0176E-11	7.2467E-12	2.7272E-12	1.2139E-14
33	1.2523E-09	7.9367E-11	2.9103E-11	5.4275E-12	2.0740E-12	9.4355E-15
34	1.2139E-09	8.7721E-11	3.3133E-11	6.3877E-12	2.4783E-12	1.1524E-14
35	7.4402E-10	6.1417E-11	2.3901E-11	4.7643E-12	1.8769E-12	8.9207E-15
36	5.9514E-10	5.5254E-11	2.2078E-11	4.5334E-12	1.8103E-12	8.7734E-15
37	4.4562E-09	4.1065E-10	1.4836E-10	3.5186E-11	1.2341E-11	3.7419E-14
38						
39						
40		1.0806E-11	3.5263E-12	9.2520E-13	3.7951E-13	1.5251E-15
41		1.3946E-11	4.9172E-12	9.8241E-13	3.7357E-13	3.0715E-15
42		1.5054E-11	5.3699E-12	1.2539E-12	5.5050E-13	5.9599E-15
43		1.9684E-11	7.8191E-12	1.8073E-12	6.8073E-13	7.3452E-15
44		2.7506E-11	9.2258E-12	1.8201E-12	7.2600E-13	6.5805E-15
45		1.9690E-11	6.2952E-12	1.3483E-12	5.1534E-13	3.8668E-15
46		5.3116E-11	1.8719E-11	4.6257E-12	1.8648E-12	8.4719E-15
47		6.6243E-11	2.3074E-11	5.1477E-12	1.5476E-12	9.1278E-15
48		6.8889E-11	2.1528E-11	4.1712E-12	1.4238E-12	1.0744E-14
49		5.5377E-11	1.7767E-11	3.2336E-12	1.1306E-12	8.7471E-15
50		1.0607E-10	3.5780E-11	7.1659E-12	2.6939E-12	1.8561E-14
51		1.2145E-10	4.2194E-11	8.5296E-12	3.1111E-12	2.1236E-14
52						
53						
54						
55						
56						
57						
58						

APPENDIX III : DREO-calculated neutron and gamma-ray multi-group spectra (units of particles per square centimetre per group) in the DLC-31 data library structure, at a detector height of 2 metres above ground.

Group	100 m	170 m	300 m	400 m	1100 m
1	.0000E 00	.0000E 00	.0000E 00	.0000E 00	.0000E 00
2	4.6962E-15	1.0909E-15	1.3426E-16	4.4796E-17	8.7939E-20
3	8.9951E-15	2.0354E-15	2.4509E-16	7.5924E-17	1.1380E-19
4	8.3667E-15	1.9962E-15	2.3718E-16	7.7224E-17	1.0564E-19
5	2.8719E-14	6.6748E-15	8.2483E-16	2.9173E-16	4.6995E-19
6	3.3232E-14	7.6434E-15	9.3882E-16	3.1783E-16	5.2614E-19
7	1.1333E-13	2.6781E-14	3.5313E-15	1.2168E-15	2.6403E-18
8	2.2685E-13	5.4634E-14	7.5531E-15	2.6620E-15	6.1425E-18
9	5.0831E-13	1.2599E-13	1.8725E-14	6.6665E-15	1.9376E-17
10	8.4730E-13	2.1576E-13	3.2930E-14	1.1813E-14	4.1457E-17
11	1.3488E-12	3.3806E-13	4.7900E-14	1.6763E-14	5.0326E-17
12	3.5288E-12	9.2987E-13	1.4784E-13	5.2423E-14	2.0263E-16
13	1.2177E-11	3.2303E-12	5.1142E-13	1.8511E-13	8.0058E-16
14	3.3535E-12	1.1134E-12	2.0188E-13	6.8021E-14	5.0235E-16
15	1.1616E-11	2.9435E-12	4.2016E-13	1.4459E-13	5.8717E-16
16	3.2399E-11	8.0999E-12	1.0032E-12	2.9511E-13	7.9251E-16
17	4.0603E-11	1.2466E-11	1.9136E-12	6.0035E-13	2.0415E-15
18	7.6874E-12	2.3852E-12	4.2122E-13	1.3518E-13	4.9932E-16
19	4.7251E-11	1.5520E-11	2.5093E-12	7.6472E-13	2.5962E-15
20	1.1094E-10	3.7230E-11	6.4075E-12	1.8888E-12	5.7037E-15
21	1.8975E-10	7.0966E-11	1.2383E-11	3.5404E-12	1.3658E-14
22	2.5706E-10	8.9100E-11	1.4736E-11	4.7824E-12	1.9574E-14
23	5.4677E-11	2.1108E-11	3.6786E-12	1.1553E-12	5.1805E-15
24	7.6831E-11	3.3581E-11	6.6812E-12	1.9222E-12	1.0028E-14
25	5.6861E-11	2.5403E-11	5.4219E-12	1.5945E-12	9.1853E-15
26	8.7712E-12	3.9471E-12	8.4053E-13	2.4847E-13	1.4700E-15
27	4.7286E-11	2.2062E-11	4.7384E-12	1.4910E-12	8.7528E-15
28	5.9869E-11	2.8804E-11	6.3438E-12	2.0894E-12	1.3208E-14
29	4.8162E-11	2.3864E-11	5.3550E-12	1.7077E-12	1.1663E-14
30	3.4301E-11	1.7212E-11	3.9774E-12	1.2359E-12	8.8131E-15
31	7.3775E-11	3.7429E-11	8.9257E-12	2.8537E-12	2.2286E-14
32	4.8596E-11	2.4843E-11	6.0413E-12	1.9341E-12	1.6349E-14
33	3.6972E-11	1.9029E-11	4.6501E-12	1.5330E-12	1.3462E-14
34	4.3696E-11	2.2695E-11	5.4547E-12	1.8260E-12	1.6616E-14
35	3.2483E-11	1.6963E-11	4.0299E-12	1.3739E-12	1.2892E-14
36	2.9846E-11	1.5538E-11	3.7086E-12	1.3412E-12	1.1981E-14
37	3.3050E-10	1.4886E-10	3.0704E-11	1.1717E-11	9.3841E-14
38	7.5727E-13	3.4621E-13	1.0709E-13	4.9151E-14	1.3570E-15
39	2.1204E-12	7.3873E-13	1.7448E-13	7.5775E-14	1.5728E-15
40	5.0059E-12	1.9658E-12	4.1541E-13	1.6233E-13	2.1570E-15
41	4.4449E-12	1.7632E-12	3.9415E-13	1.6318E-13	2.4586E-15
42	7.2133E-12	2.9257E-12	7.6188E-13	3.3620E-13	6.3218E-15
43	1.3576E-11	5.0367E-12	1.0520E-12	4.0300E-13	5.1489E-15
44	2.0821E-11	7.3842E-12	1.4989E-12	5.6747E-13	6.4412E-15
45	1.4948E-11	3.9173E-12	7.8628E-13	3.0824E-13	3.3632E-15
46	6.1826E-11	2.1717E-11	4.2650E-12	1.5354E-12	1.1164E-14
47	5.0399E-11	1.2325E-11	2.2575E-12	8.4096E-13	6.6995E-15
48	8.2409E-11	1.7551E-11	3.3014E-12	1.1721E-12	9.8278E-15
49	6.7997E-11	1.7780E-11	2.8197E-12	1.0851E-12	9.3815E-15
50	8.8519E-11	2.4029E-11	4.2839E-12	1.8526E-12	1.5491E-14
51	7.1790E-11	2.3841E-11	4.6412E-12	1.8309E-12	1.5184E-14
52	1.6827E-10	6.8161E-11	1.2737E-11	4.9315E-12	4.3934E-14
53	1.1505E-10	4.8714E-11	9.9713E-12	3.6639E-12	3.1510E-14
54	1.0891E-10	4.7691E-11	1.0683E-11	3.8279E-12	3.4952E-14
55	9.1189E-11	4.3670E-11	1.1248E-11	4.0723E-12	3.8432E-14
56	2.0769E-11	1.0549E-11	2.9762E-12	1.0951E-12	1.0406E-14
57	1.4097E-12	7.1565E-13	2.1346E-13	7.9384E-14	8.0644E-16
58	1.2869E-14	6.8029E-15	2.0261E-15	7.5468E-16	7.7722E-18

APPENDIX IV : 252-Californium neutron and gamma-ray spectra.

In order to provide neutron and gamma-ray spectra to which other groups such as WWD and APRD may compare corresponding results, DREO measurements of the APRD 252-californium source are presented herein.

Measurements were made at a source-to-detector distance of 2 metres, with both source and detector at a height of 119 cm above the asphalt road just beyond the APRD trailer tunnel. Observation time was 1800 seconds, during which the most active channel (high gain gamma-ray) suffered a dead-time loss of 17 seconds. The date of observation was 16 Oct 1980.

Unfolded neutron and gamma-ray spectra are shown in Figures 26 and 27 respectively. Both are normalized to particles per square centimetre - second, with the neutron spectrum plotted in such a way as to make the familiar Maxwellian shape appear as a straight line. The Maxwellian temperature determined from the slope of this line is 1.40 MeV, consistent with other observations (12).

The gamma-ray spectrum exhibits two discrete lines at approximately 1.3 and 2.7 MeV which are not due to the fission of 252-californium itself, but which probably result from the beta-decay of 24-sodium produced by the (n,alpha) reaction on 27-aluminum. The photon energies expected from this decay are 1.369 and 2.754 MeV (in equal intensity), consistent with the above observation. The source of aluminum is likely to be the encapsulation of the californium source.

A total neutron flux of 53.0 neutrons per square-centimetre - second is obtained above the NE-213 threshold of 600 keV. The corresponding total gamma-ray flux above 300 keV was measured as 169 photons per square-centimetre - second. It should be noted that these fluxes include the ground-scattered component, as no shadow-bar background measurement was made. For this reason comparison of the measured source strengths with the calibrated value would be inappropriate. However, previous DREO measurements in 1978 of an NBS-calibrated source, including ground-scattering correction, indicated a total intensity agreeing to within 3 % of calibration, with a similar spectral shape as presently observed.

Neutron and gamma-ray kerma-rates recorded above the NE-213 thresholds were 1.65E-7 and 8.57E-8 rads per second respectively, with estimated experimental errors of 10 %.

It is hoped that measurements by WWD and APRD under similar conditions will help to resolve the causes of differences in spectral determinations between the three groups noted earlier in this report.
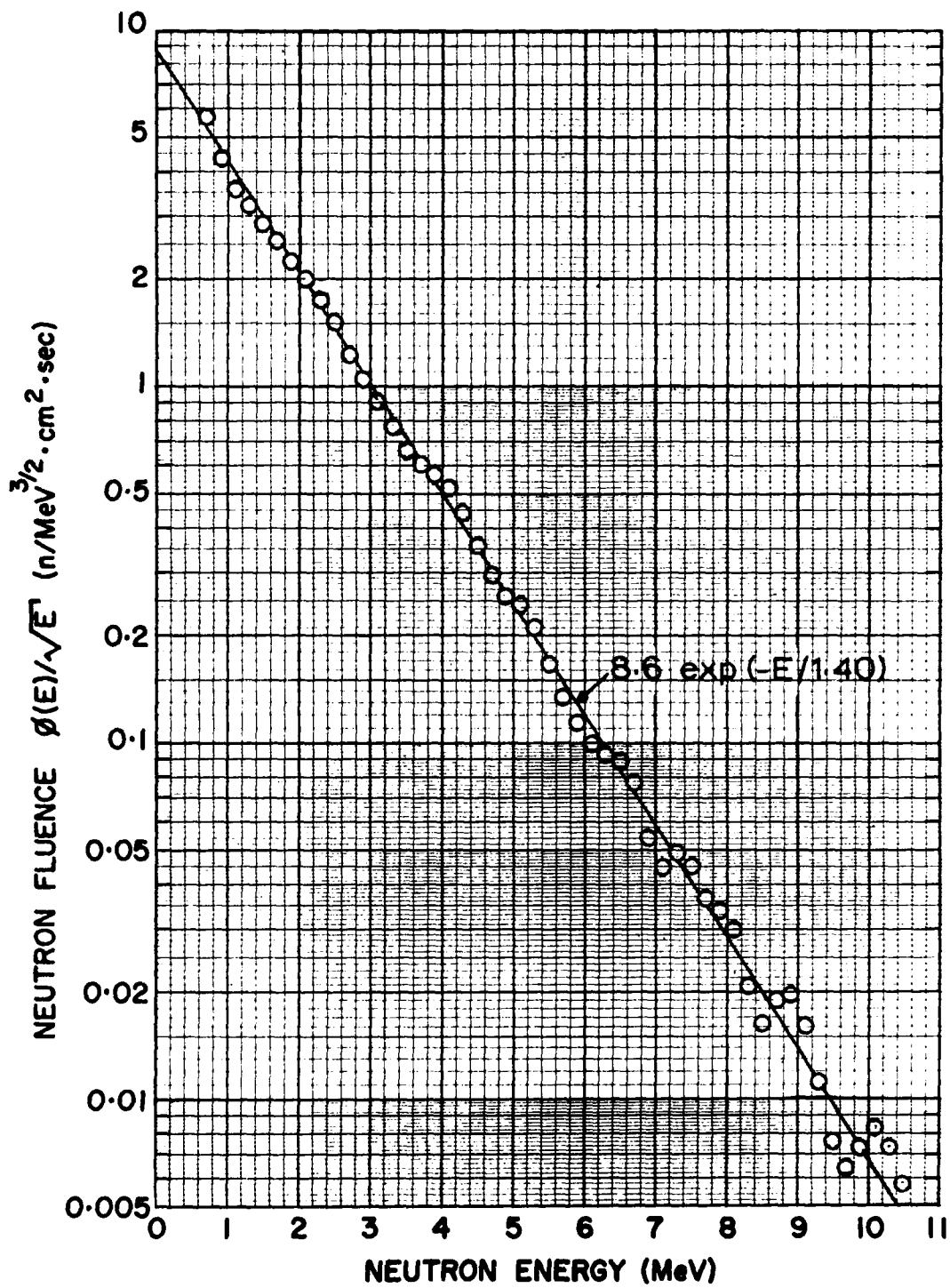
Figure 26 : Neutron spectrum measured by DREO at a distance of
two metres from the APRD 252-californium source.
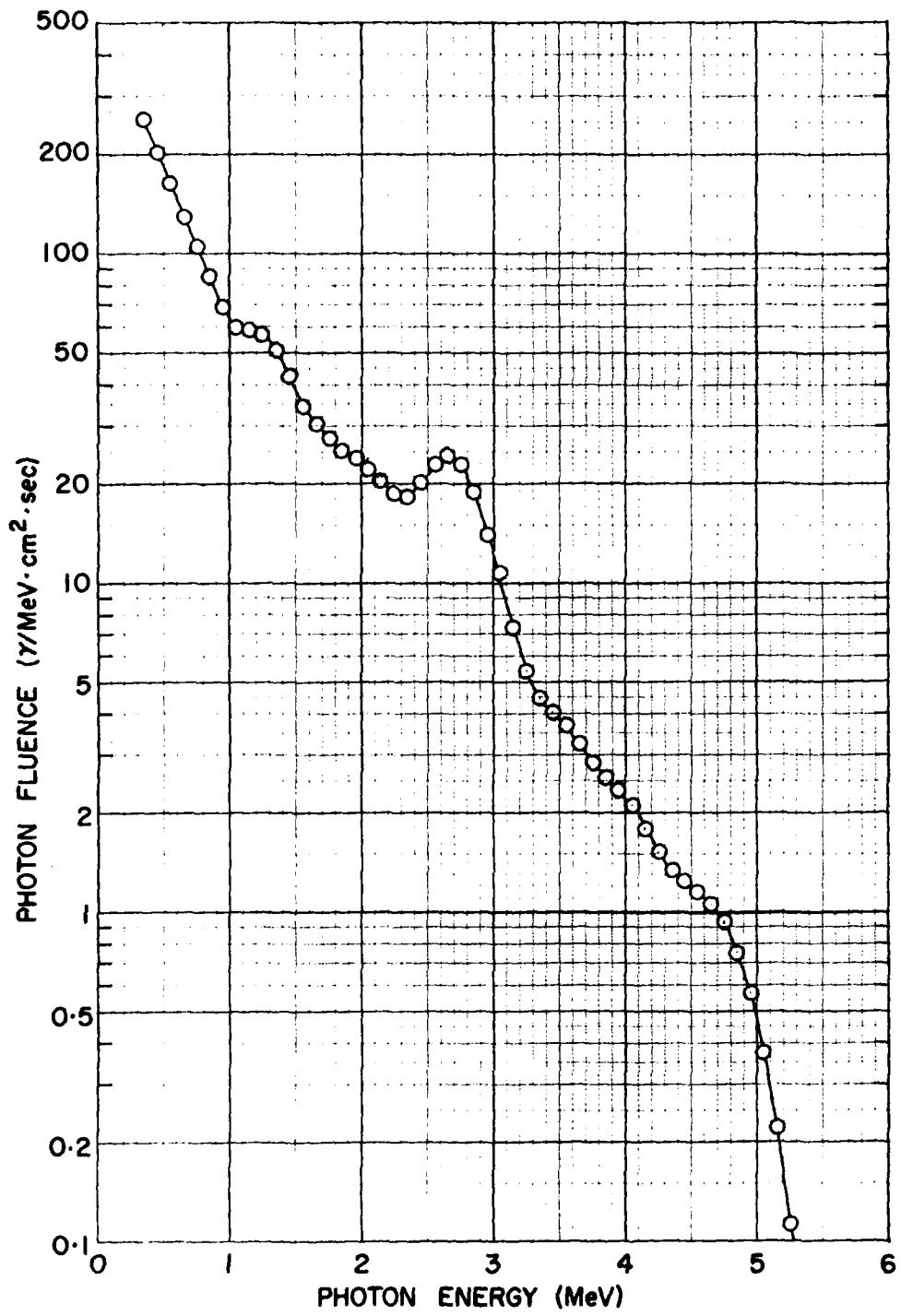
Figure 27 : Gamma-ray spectrum measured by DREO at a distance
of two metres from the APRD 252-californium source.

REFERENCES

1. H.A. Robitaille, "Initial Nuclear Radiation Environments due to Tactical Nuclear Weapons Detonated in Air-over-Ground and Air-over-Sea Geometries", DREO Report No R808, July 1979, Department of National Defence, Canada

2. A.H. Kazi, "Fast-Pulse Reactor Operation with Reflector Control and a 106-mm-diam Glory Hole", Nuclear Science and Engineering, 60(1976)62-73.

3. A.H. Kazi, et al, "Measurements of the Free Field Radiation Environment at the APRD Reactor", TECOM Report No APG-MT-5279, July 1979, US Army

4. F.P. Szabo, "A Fast-Neutron Spectrometer", DREO Report No R637, July 1971, Department of National Defence, Canada

5. H.A. Robitaille, "Rapid, On-Line Matrix Unfolding of Fast-Neutron Spectroscopic Data from Organic Scintillators", Third Symposium on Neutron Dosimetry in Biology and Medicine, Neuherberg/Munchen, May 1977, Commission of the European Communities, Luxembourg

6. N.A. Lurie, L. Harris, J.C. Young, "Calculation of Gamma-Ray Response Matrix for 5-cm NE-213 Organic Liquid Scintillation Detectors", Nuclear Instruments and Methods, 129(1975)543-555.

7. D.E. Bartine, et al, "Production and Testing of the DNA Few Group Cross-Section Library", Report No ORNL-TM-4840, October 1975, Oak Ridge National Laboratory, Tennessee

8. Model RS-P1-0809-101, Reuter-Stokes Inc., Cleveland, Ohio

9. C.K. Hargrove and K.W. Gieger, "A New Thermal Neutron Flux Density Standard", Canadian Journal of Physics, 42(1964)1593-1604.

10. K.W. Gieger and D.W.O. Rogers, "Time Dependence of the Thermal Neutron Flux Density in the Canadian Flux Standard", Metrologia 13(1977)67-68

11. L. Schanzler, et al, "Measurements of the Free Field Radiation Environments at the APRD Reactor", WWD Report No 27, February 1979, Wehrwissenschaftliche Dienststelle der Bundeswehr fur ABC-Schutz, Munster, FRG

12. L. Green, J.A. Mitchell, and N.M. Steen, "The Californium-252 Fission Neutron Spectrum from 0.5 to 13 MeV", Nuclear Science and Engineering 50(1973)257-272

13. F. W. Bucholz, L. Schanzler, S. Stuker, G. Trumbagel and M. Weiner, "Californium Liquid Air Tank Experiment", WWD Report No. 33, December 1976, Wehrwissenschaftliche Dienststelle der Bundeswehr fur ABC-Schutz, Munster, FRG

14. R.E. Textor and V.V. Verbinski, "O5S, A Monte-Carlo Code for Calculating Pulse Height Distributions Due to Monoenergetic Neutrons Incident on Organic Scintillators", ORNL Report No. 4160 (1968), Oak Ridge National Laboratory, Tennessee

46

15. A.H. Kazi, Private communication, 20 Nov 1980

16. A.H. Kazi, C.R. Heimbach, L. Schanzler, J.V. Pace III, A.E. Rainis, "Comparison of Experimental Radiation Transport with Calculation", Transactions of the American Nuclear Society, San Francisco 11-15 Nov 1979, TANSAO 33 (1979)706-707

17. F.R. Mynatt, et al, "The DOT-III Two-Dimensional Discrete Ordinates Transport Code", ORNL Report No TM-4280, June 1973, Oak Ridge National Laboratory, Tennessee

DOCUMENT CONTROL DATA - R & D

(Security classification of title, body of abstract and indexing annotation must be entered when the overall document is classified)

1. ORIGINATING ACTIVITY DEFENCE RESEARCH ESTABLISHMENT OTTAWA DEPARTMENT OF NATIONAL DEFENCE OTTAWA, ONTARIO, CANADA K1A 0Z4	2a. DOCUMENT SECURITY CLASSIFICATION UNCLASSIFIED
	2b. GROUP n/a

3. DOCUMENT TITLE

A COMPARISON OF MEASURED AND CALCULATED AIR-TRANSPORTED RADIATION FROM A FAST, UNSHIELDED NUCLEAR REACTOR

4. DESCRIPTIVE NOTES (Type of report and inclusive dates)

Technical Report No. DREO R 835 (1980)

5. AUTHOR(S) (Last name, first name, middle initial)

ROBITAILLE, H. Alan and HOFFARTH, Bernard E.

6. DOCUMENT DATE DECEMBER 1980	7a. TOTAL NO. OF PAGES 46	7b. NO. OF REFS 17
8a. PROJECT OR GRANT NO SPN 11A10-1	9a. ORIGINATOR'S DOCUMENT NUMBER(S) DREO R-835	
8b. CONTRACT NO n/a	9b. OTHER DOCUMENT NO.(S) (Any other numbers that may be assigned this document) n/a	

10. DISTRIBUTION STATEMENT

Unlimited

11. SUPPLEMENTARY NOTES n/a	12. SPONSORING ACTIVITY CRAD(DREO)

13. ABSTRACT

Neutron and gamma-ray spectra have been measured at various distances up to 1100 metres from the fast-neutron reactor of the U.S. Army Pulse Radiation Division (Materiel Testing Directorate, Aberdeen Proving Ground, Md.) The spectra were obtained at a height of two metres above the air-ground interface and are compared to previous measurements performed by two other research laboratories, and also to the results of theoretical predictions based on two-dimensional discrete-ordinates transport theory.

Integral quantities such as partial and total radiation kermas are generally in good agreement, however the theoretical calculations tend to predict somewhat softer neutron spectra than are observed experimentally.

DSIS

Security Classification

KEY WORDS

RADIATION
NEUTRON
GAMMA-RAY
NUCLEAR REACTOR
NUCLEAR WEAPON
DOSE
SPECTRA

INSTRUCTIONS

1. ORIGINATING ACTIVITY. Enter the name and address of the organization issuing the document.

2a. DOCUMENT SECURITY CLASSIFICATION. Enter the overall security classification of the document including special warning terms whenever applicable

2b. GROUP. Enter security reclassification group number. The three groups are defined in Appendix 'M' of the DRB Security Regulations.

3. DOCUMENT TITLE. Enter the complete document title in all capital letters. Titles in all cases should be unclassified. If a sufficiently descriptive title cannot be selected without classification, show title classification with the usual one-capital-letter abbreviation in parentheses immediately following the title.

4. DESCRIPTIVE NOTES. Enter the category of document, e.g. technical report, technical note or technical letter. If appropriate, enter the type of document, e.g. interim, progress, summary, annual or final. Give the inclusive dates when a specific reporting period is covered.

5. AUTHOR(S). Enter the name(s) of author(s) as shown on or in the document. Enter last name, first name, middle initial. If military, show rank. The name of the principal author is an absolute minimum requirement.

6. DOCUMENT DATE. Enter the date (month, year) of Establishment approval for publication of the document.

7a. TOTAL NUMBER OF PAGES. The total page count should follow normal pagination procedures, i.e. enter the number of pages containing information

7b. NUMBER OF REFERENCES. Enter the total number of references cited in the document

8a. PROJECT OR GRANT NUMBER. If appropriate, enter the applicable research and development project or grant number under which the document was written

8b. CONTRACT NUMBER. If appropriate, enter the applicable number under which the document was written.

9a. ORIGINATOR'S DOCUMENT NUMBER(S). Enter the official document number by which the document will be identified and controlled by the originating activity. This number must be unique to this document.

9b. OTHER DOCUMENT NUMBER(S). If the document has been assigned any other document numbers (either by the originator or by the sponsor), also enter this number(s).

10. DISTRIBUTION STATEMENT. Enter any limitations on further dissemination of the document, other than those imposed by security classification, using standard statements such as:

   (1) "Qualified requesters may obtain copies of the document from their defence documentation center.

   (2) "Announcement and dissemination of this document is not authorized without prior approval from originating activity."

11. SUPPLEMENTARY NOTES. Use for additional explanatory notes.

12. SPONSORING ACTIVITY. Enter the name of the departmental project office or laboratory sponsoring the research and development. Include address.

13. ABSTRACT. Enter an abstract giving a brief and factual summary of the document, even though it may also appear elsewhere in the body of the document itself. It is highly desirable that the abstract of classified documents be unclassified. Each paragraph of the abstract shall end with an indication of the security classification of the information in the paragraph (unless the document itself is unclassified) represented as (TS), (S), (C), (R), or (U).

The length of the abstract should be limited to 20 single-spaced standard typewritten lines, 7½ inches long

14. KEY WORDS: Key words are technically meaningful terms or short phrases that characterize a document and could be helpful in cataloging the document. Key words should be selected so that no security classification is required. Identifiers, such as equipment model designation, trade name, military project code name, geographic location, may be used as key words but will be followed by an indication of technical context

END

DATE
FILMED

10-81

DTIC